

# New Insights on the QSO Radio-Loud/Radio-Quiet Dichotomy: SDSS Spectra in the Context of the 4D Eigenvector1 Parameter Space

S. Zamfir<sup>1\*</sup>, J. W. Sulentic<sup>1</sup> and P. Marziani<sup>2</sup>

<sup>1</sup>*Department of Physics and Astronomy, University of Alabama, Box 970324, Tuscaloosa, AL 35487, USA*

<sup>2</sup>*INAF-Osservatorio Astronomico di Padova, Vicolo dell'Osservatorio 5, I-35122 Padova, Italy*

4 April 2008

## ABSTRACT

We search for a dichotomy/bimodality between Radio Loud (RL) and Radio Quiet (RQ) Type 1 Active Galactic Nuclei (AGN). We examine several samples of SDSS QSOs with high S/N optical spectra and matching FIRST/NVSS radio observations. We use the radio data to identify the weakest RL sources with FRII structure to define a RL/RQ boundary which corresponds to  $\log L_{1.4\text{GHz}} = 31.6 \text{ ergs s}^{-1} \text{ Hz}^{-1}$ . We measure properties of broad line H $\beta$  and FeII emission to define the optical plane of a 4DE1 spectroscopic diagnostic space. The RL quasars occupy a much more restricted domain in this optical plane compared to the RQ sources, which a 2D Kolmogorov-Smirnov test finds to be highly significant. This tells us that the range of BLR kinematics and structure for RL sources is more restricted than for the RQ QSOs, which supports the notion of dichotomy. FRII and CD RL sources also show significant 4DE1 domain differences that likely reflect differences in line of sight orientation (inclined vs. face-on respectively) for these two classes. The possibility of a distinct Radio Intermediate (RI) population between RQ and RL source is disfavored because a 4DE1 diagnostic space comparison shows no difference between RI and RQ sources. We show that searches for dichotomy in radio vs. bolometric luminosity diagrams will yield ambiguous results mainly because in a reasonably complete sample the radio brightest RQ sources will be numerous enough to blur the gap between RQ and RL sources. Within resolution constraints of NVSS and FIRST we find no FRI sources among the broad line quasar population.

**Key words:** galaxies: active, (galaxies:) quasars: emission lines, (galaxies:) quasars: general

## 1 INTRODUCTION

A much debated problem in AGN studies involves the possibility of a real physical dichotomy between radio-loud (RL) and radio-quiet (RQ) QSOs. The low fraction of RL sources - on average  $\sim 5\text{-}25\%$  (e.g. Kellermann et al. 1989; Padovani 1993; Kellermann et al. 1994; Jiang et al. 2007) depending on the adopted definition of radio-loudness - and its dependence on redshift and optical luminosity (e.g. Peacock et al. 1986; Miller et al. 1990; Visnovsky et al. 1992; Padovani 1993; Hooper et al. 1995; Goldschmidt et al. 1999; Jiang et al. 2007) add to the difficulty of defining statistically meaningful samples of QSOs with which to identify potentially bimodal properties.

Another complication is introduced by the fact that some good fraction of RQ sources share common properties with the RL quasars; for example: a) about 30-40% of RQ QSOs are spec-

troscopically similar to RL (e.g. Sulentic et al. 2000a, and present study) and b) both QSO types are capable of producing radio jets. RQ jets typically extend over scales of a few parsecs up to kiloparsecs (e.g. Blundell & Beasley 1998; Kukula et al. 1998; Ulvestad et al. 2005; Leipski et al. 2006)<sup>1</sup> and RL much larger scales with higher radio power (e.g. Rawlings & Saunders 1991; Miller et al. 1993). Potential bimodal properties might be hiding behind such similarities.

The very definition of radio-loudness is rather “loose” with continued disagreement over the empirical RL/RQ boundary. Over the last few decades a couple of possible boundary criteria have been proposed based on: Criterion 1 - radio power (Miller et al. 1990) and Criterion 2 - radio/optical flux density ratio. Criterion 2 involves the much used Kellermann factor  $R_K$  (radio flux density at

<sup>1</sup> However Ulvestad et al. (2005) report deep lower frequency VLBI observations of several RQ objects studied by Blundell & Beasley (1998) and do not confirm the presence of jet-related structure.

\* E-mail: zamfi001@bama.ua.edu

6cm normalized to B-band flux density). Kellermann et al. (1989) suggested  $R_K = 10$  for the RL-RQ boundary in the Palomar-Green (PG) sample of QSOs (Schmidt & Green 1983; Green et al. 1986; Boroson & Green 1992) and many studies have adopted this value. Others have suggested that different nominal  $R_K$  limits for radio steep- and flat-spectrum sources would eliminate the confusion introduced by a fixed value of 10 (Falcke et al. 1996a). Sikora et al. (2007) propose another kind of quantitative distinction for RL AGNs based on  $R_K$  as a function of Eddington ratio (see their section 4.1). This definition might be relevant if one includes FRI sources and LINERs that do not show broad lines.

There are several different surrogate definitions of  $R_K$  in literature involving radio measures at various frequencies and optical (B-band or i-band), UV or even X-ray measures (e.g. Kellermann et al. 1989; Stocke et al. 1992; Ivezić et al. 2002; Terashima & Wilson 2003; Jester et al. 2005a; Wang et al. 2006; Jiang et al. 2007), which obviously complicates the comparison of different studies.

It is still unclear whether one of the two criteria is more physically significant. Studies like Miller et al. (1990) promote the radio power as a more fundamental discriminator, while others argue in favor of the second criterion, which relates the radio properties to other regimes of energy output. Moreover, while some galactic nuclei qualify as radio-loud based on one boundary criterion they fail to do so when using the other. A good example (Ho & Peng 2001) involves a sample of bright Seyfert nuclei where as many as  $\sim 60\%$  of the sources are RL using  $R_K > 10$  (adopting a “nuclear” radio-optical ratio), but only one would satisfy the condition of  $L(6\text{cm}) > 10^{25} \text{ W Hz}^{-1} \text{ sr}^{-1}$  (Miller et al. 1990). The conclusions in Ho & Peng (2001) are provocative in terms of both the radio loud fraction and the fact that many of their so-called “radio-loud” would be hosted by spiral galaxies, a rather different result compared to more luminous samples analyzed in studies like e.g. Taylor et al. (1996), McLure et al. (1999), Dunlop et al. (2003). Laor (2003) explains (based on the results of Xu et al. 1999) that  $R_K$  is Luminosity-dependent and one should rather use  $R_K \propto L^{-0.5}$  to separate RLs from RQs. The  $R_K=10$  suggested by Kellermann et al. (1989) for luminous samples ( $M_B \sim -26$ ) is not a valid choice for RL boundary for low luminosity samples (e.g. Ho & Peng 2001). Nonetheless,  $R_K$  retains its heuristic value because it offers a scaling relation between nonthermal and thermal mechanisms at work in AGN. After all, for theoretical models of accretion disk it is preferable to use dimensionless quantities like the Eddington-scaled luminosity and accretion rate (although there may be different scaling relations for jets, disk, corona luminosity with accretion rate and black hole mass, e.g. Kording et al. 2006a).

Thus, we face the problem of labeling objects differently depending on the adopted definition of boundary criterion, which complicates the integration of different results into a more general picture. A further problem involves the combination of radio and optical flux measures (the latter being susceptible to internal extinction) that can introduce serious selection effects and biases at different redshifts thus making  $R_K$  a problematic radio-loudness indicator for statistical purposes. These aspects reinforce the necessity of alternative approaches toward a consistent definition of *radio-loud*. We need a more standardized definition.

Different studies over the last decade report contradictory results regarding the question of a bimodal distribution of QSOs in terms of radio-loudness. Recent SDSS-based studies (e.g. Ivezić et al. 2002; White et al. 2007) defend the reality of bimodality for QSO distribution using histograms of radio/optical(UV) ratios. The latter study shows a significant dip at  $R_K \sim 30-40$  (see

their Figure 15). They employ image stacking to lower the detection limit of FIRST to nano-Jy levels and their final sample includes over 41000 sources. A bimodal distribution is found by Liu et al. (2006) in terms of  $R_K$  corrected for orientation (although with a heterogeneous sample). Their Figure 9 shows a cutoff in the RL population in the range  $\log R_K = 1.5-2.0$ . There are at the same time many studies that question the reality of bimodality (Falcke et al. 1996a; White et al. 2000; Brotherton et al. 2001; Lacy et al. 2001; Cirasualo et al. 2003a; Cirasoulo et al. 2003b). Falcke et al. (1996a), Lacy et al. (2001), Brotherton et al. (2001) propose a population of Radio Intermediate sources (RI) that might bridge the gap between RL and RQ. Clearly, the RL/RQ problem is far from resolved reflected in the lack of consensus on how to consistently define a radio-loud sample or prove the existence of a physical dichotomy.

Even if the distribution of radio-loudness measures for a sample of RL and RQ sources may not exhibit bimodality, we showed that they may represent two distinct classes of AGN, based on spectroscopic measures (Sulentic et al. 2003). The present study attempts to provide more robust empirical support to this alternative approach. This paper also shows that the picture of “dichotomy” is significantly distorted by mixing bright and faint QSO samples when we are flux-limited in both optical and radio regimes.

We recently considered (Sulentic et al. 2003) a third RL/RQ boundary criterion (Criterion 3) based on the classical radio morphology. Double-lobe FR II morphology (Fanaroff & Riley 1974) is the most common type observed in broad line emitting RL quasars. FRI morphology is very rare among broad-line AGN, e.g. 3C120, E1821+643 (Blundell & Rawlings 2001) and SDSS J104022.79+444936.7 (Heywood et al. 2007). The latter reference suggests that FRI morphology may become more common among broad-line quasars beyond  $z \sim 1.0$ . In a simple orientation unification scenario (Urry & Padovani 1995) core-dominated (CD) RL sources are interpreted as FR II sources viewed with radio jet axis aligned close to our line of sight. If this scenario is valid then the CD counterparts of any FR II population will be on average more radio luminous due to relativistic boosting effects (e.g. Orr & Browne 1982; Scheuer 1987; Barthel 1989; Jackson & Wall 1999). We adopted the weakest (assumed unboosted) FR II sources in our sample to define the lower boundary of the RL phenomenon. This also allowed us to redefine the boundary in terms of Criterion 1 ( $\log P_{6\text{cm}} \sim 32.0 \text{ erg s}^{-1} \text{ Hz}^{-1}$ ) and Criterion 2 ( $R_K \sim 70$ ).

In the present study we reiterate the idea that a robust definition of a radio-loud quasar can be formulated only if radio-morphology is taken into account. More specifically the FR IIs should be considered the parent population of RL quasars (e.g. Orr & Browne 1982; Scheuer 1987; Barthel 1989; Taylor et al. 1996; Jackson & Wall 1999). This is also supported by the recent confirmation that the shape of the observed luminosity function of FR II radio galaxies is the same as the intrinsic luminosity function of RL quasars (Liu & Zhang 2007). In other words, the radio weakest FR II structures should dictate the empirical boundary between RL quasars and the rest of the QSO population. We therefore defined a sample of RL quasars using the radio luminosity coupled with the radio morphology in order to avoid the perviously discussed problems associated with  $R_K$  (see also Wadadekar & Kembhavi 1999).

We have been exploring a 4D parameter space (4DE1; Sulentic et al. 2000a,b; Marziani et al. 2001, 2003a,b; Sulentic et al. 2007) that serves as a spectroscopic unifier/discriminator for all broad emission line AGNs (Type 1). Our principal parameters involve measures of: 1) full width at half

maximum of broad  $H\beta$  (FWHM  $H\beta$ ), 2) equivalent width ratio of optical FeII ( $\lambda 4570\text{\AA}$  blend) and broad  $H\beta$ ,  $R_{FeII} = W(\text{FeII } \lambda 4570\text{\AA})/W(H\beta)$ , 3) the soft X-ray photon index ( $\Gamma_{soft}$ ) and 4) CIV  $\lambda 1549\text{\AA}$  broad line profile velocity displacement at half maximum,  $c(1/2)$ . The “Introduction” of Sulentic et al. (2007) explains how this parameter space evolved from various pioneering works. One enormous advantage of this parameter space formulation is its weak or absent dependence on source luminosity (Sulentic et al. 2000a, 2004). Armed with our improved definition of the lower boundary for RL activity in quasars we compared their 4DE1 properties with RQ sources. We found that most RL sources show a much restricted domain space occupation within the optical parameter plane of 4DE1 (FWHM  $H\beta$  vs.  $R_{FeII}$ ) compared to the RQ majority (Sulentic et al. 2003).

Although the results presented in 2003 provided compelling support for RL-RQ bimodality, the adopted sample was rather heterogeneous, incomplete and included many sources with measures derived from marginal S/N spectra. With the advent of the SDSS database it becomes possible to select a large and much more complete ( $\sim 90\%$ )<sup>2</sup> sample of AGN with uniformly high resolution and S/N optical spectra. A further advantage involves the larger wavelength interval 3800-9200 $\text{\AA}$  sampled by SDSS. This is complemented by uniform radio survey data from FIRST<sup>3</sup> designed to match the SDSS sky coverage and NVSS survey<sup>4</sup>.

The value of studying the radio-loud phenomenon within the 4DE1 context is at least twofold: 1) it compares RL and RQ sources in a parameter space defined by measures with no obvious dependence on the radio properties (Marziani et al. 2003b) and 2) it allows us to make predictions about the probability of radio loudness for any population of QSOs with specific optical (or UV) spectroscopic properties.

The paper is organized as follows: § 2 presents the sample selection and the RL definition based on radio morphology and radio luminosity. § 3 presents the 4DE1 optical measures. § 4 includes differences in RQ, RI and RL source occupation within 4DE1. § 5 offers a discussion on the RL/RQ dichotomy based on L-dependent diagrams. In § 6 and § 7 we discuss the fraction of RL quasars and the probability of radio-loudness within the 4DE1 optical plane. The last two sections are dedicated to discussions and conclusions. Throughout this paper we use  $H_0 = 70 \text{ km s}^{-1} \text{ Mpc}^{-1}$ ,  $\Omega_M = 0.3$  and  $\Omega_\Lambda = 0.7$ .

## 2 DEFINING A POPULATION OF RADIO-LOUD QUASARS

We consider any AGN that shows broad (Balmer) emission lines as “QSO” regardless of its intrinsic luminosity (or absolute magnitude). This is why we generated our own sample of SDSS QSOs (from Data Release 5 of SDSS; Adelman-McCarthy et al. 2007) instead of extracting it from the vetted catalog of Schneider et al. (2007) that is limited to sources with absolute magnitude  $M_i \leq -22.0$ . Sample size is driven by the following goals: i) a sample of

high quality spectra suitable for 4DE1 spectroscopic analysis, ii) as complete as possible sample of RL quasars, iii) a large enough sample of RQ quasars with reliable 4DE1 measures so that we can define the RQ zone of occupation, iv) a representative sample of so-called RI sources and v) source-by-source evaluation to avoid the pitfalls (e.g. radio/optical misidentifications, misclassifications) of automated processing. Our approach is based on careful examination of each optical spectrum in order to confirm the presence of broad lines. All FIRST/NVSS (20cm/1.4GHz) radio maps were visually examined in order to evaluate radio morphology, resolve ambiguous cases and obtain the correct integrated (total) radio flux density.

**OPTICAL SELECTION:** We restricted source selection to  $z \leq 0.7$  so that  $H\beta$  and adjacent spectral regions of interest (used to define the underlying continuum) would be accessible. We selected our sample in several steps. Step 1 selected all SDSS DR5 quasars with  $\text{psf } g < 17.0$  ( $n=333$  QSOs with 34 RL). This selection was motivated by the need for high S/N spectra from which 4DE1 parameters could be reliably measured. Step 2 extended this limit to  $\text{psf } g=17.5$  ( $n=806$  QSOs with 76 RL). This extension was motivated by the desire to increase the RL sample. Our first two steps are based on a rather blue filter, close to BQS (Schmidt & Green 1983; Green et al. 1986; Boroson & Green 1992). Although Jester et al. (2005a) find no radio-related incompleteness for BQS-like selected samples, they point out that the apparently large fraction of RL in BQS survey is related to its rather blue filter (B-band) selection (see § 6). Having this in mind, we considered also a step 3 aimed to define a RL sample considering all QSOs brighter than  $\text{psf } i=17.5$  ( $n=1656$  QSOs with 91 RL). In Table 1 we explain which objects have been considered for the spectroscopic analysis.

We offer in Figure 1 the sources redshift distributions resulting from the two selections (based on  $\text{psf } g < 17.5$  and based on  $\text{psf } i < 17.5$ ). Selection using the g-band magnitude limit yields a sample with much more uniform redshift distribution. Not surprisingly i-band selection (much more complete) favors redder local QSOs (50% have  $z < 0.15$ ; 60% have  $z < 0.20$  and 70% have  $z < 0.25$ ), more strongly affected by host galaxy contamination and/or by the presence of  $H\alpha$  line inside i-band. There is obviously a large overlap between the samples. The census presented here also includes the objects that show broad lines narrower than  $1000 \text{ km s}^{-1}$  and are labeled “Galaxy” by the SDSS spectroscopic pipeline (see the appendix and see also Table 2). Such sources can be safely included under the generic umbrella of “QSO”. However, these objects were not included in our spectroscopically-processed sample for the following reasons: 1) limitation of our template used to extract the FeII lines from our spectra (same as used in Boroson & Green 1992) or 2) very red continua, extreme Balmer decrement, significant galaxy contamination and dramatically different  $H\alpha$  and  $H\beta$  broad lines. We also included all QSO spectra that have been assigned only a “Science Primary” index of 0<sup>5</sup>.

**RADIO SELECTION:** We used FIRST combined with NVSS to evaluate the integrated radio emission and source structure. For FIRST survey the typical rms fluctuations are 0.15 mJy, and the resolution is 5”. For NVSS survey the rms brightness fluctuations

<sup>2</sup> As defined within the SDSS project the completeness was estimated in two ways: by checking how many of the previously known QSOs are recovered and evaluating the output of target selection for simulated quasars, see Richards et al. (2002) and Vanden Berk et al. (2005)

<sup>3</sup> Faint Images of the Radio Sky at Twenty-centimeters (FIRST)- <http://sundog.stsci.edu/>; see also Becker et al. (1995)

<sup>4</sup> NRAO VLA Sky Survey (NVSS) - <http://www.cv.nrao.edu/nvss/>; see also Condon et al. (1998)

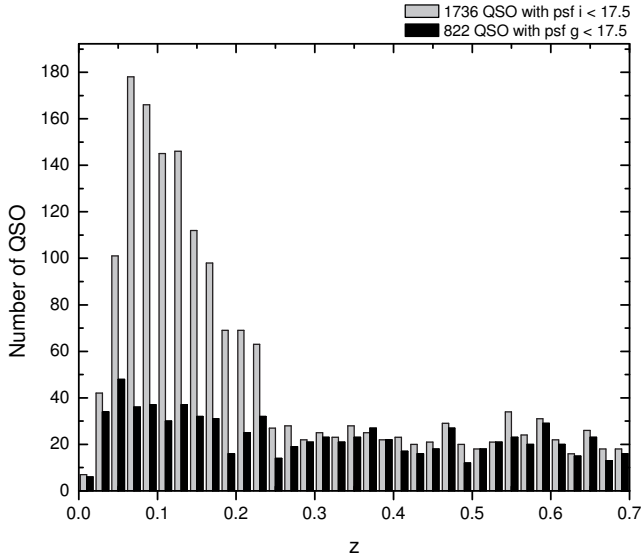
<sup>5</sup> “The SDSS SCIENCEPRIMARY flag indicates whether a spectrum was taken as a normal science spectrum (SCIENCEPRIMARY = 1) or for another purpose (SCIENCEPRIMARY = 0). The latter category contains quality assurance and calibration spectra, or spectra of objects located outside of the nominal survey area.” (Schneider et al. 2007)

**Table 1.** Samples with  $z < 0.7$  selected for spectral analysis in the Context of 4DE1.

Apparent Magnitude	$N_{total}$	$N_{RL}$	$N_{radio-detected}$	Considered for Spectral Analysis?
psf $g < 17.0$	333	34	136	all
$17.0 \leq \text{psf } g < 17.5$	473	42	122	all radio detected (either FIRST or NVSS)
psf $i < 17.5$ AND psf $g \geq 17.5$	850	19	206	only if $L_{1.4GHz} \geq 31.0 \text{ erg s}^{-1} \text{ Hz}^{-1}$ (all RI and RL)

Notes: Every QSO in the samples selected based on g-filter was examined in FIRST/NVSS radio maps.

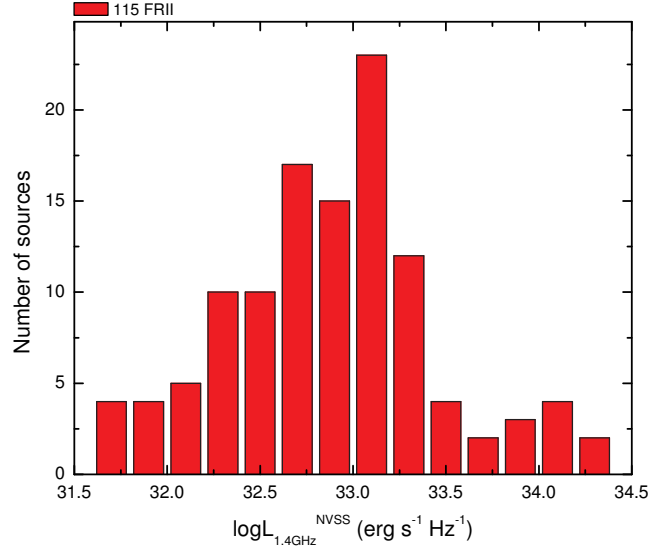
The radio properties for the sample of QSOs selected by the third set of criteria (based on i-filter) were determined in several steps: 1) we searched FIRST within  $15''$  from the optical position, then 2) all sources without a detection (or not in area covered by FIRST) were searched in NVSS around  $80''$  and finally 3) all sources that are radio-detected in either survey are examined in detail in order to get the total flux density from all components.

**Figure 1.** The distribution of QSOs apparently brighter than psf  $g = 17.5$  (black) and brighter than psf  $i = 17.5$  (light grey).

are  $0.45 \text{ mJy beam}^{-1}$ , with a  $45''$  resolution (see footnotes 3 and 4 of this paper for the sources of this technical details). Both radio maps were compared to avoid missing extended sources that might have been attenuated with FIRST. The  $45''$  beam of NVSS yields sensitivity to more extended structure and provides radio data for a few sources not observed by FIRST. We also wanted to clarify the nature of any significant discrepancies between the two surveys for specific sources.

We identified all bona fide FR II structures associated with our sample of QSOs. Two sources (SDSSJ075407.96+431610.6 and SDSSJ080131.97+473616.0) show bright cores with detached and apparently unrelated satellite sources using FIRST. NVSS shows that they are FR II with very large (Mpc-scale) radio FR II structure that reveals the satellite sources as associated hotspots. SDSS J013521.67-004402.0 is an excellent example of false FR II and false RL. At the same time not all detected double-lobed sources in a sample can be unambiguously classified as FR II. However all sources with: 1) low enough redshift, 2) a broad line spectrum (Type 1 AGN) and 3) adequate radio resolution show FR II (or hybrid e.g. HYMOR - see Gopal-Krishna & Wiita 2000) morphology. We therefore assume that all double lobed RL sources in our sample are FR II. All sources with FR II structure are assumed to be RL, while the other sources (with core or core-jet radio morphology) are considered RL only if they have the radio power  $L_{1.4GHz}$  above the threshold set by the weakest FR II.

Comparison of NVSS and FIRST flux densities for each RL

**Figure 2.** The distribution of  $\log L_{1.4GHz}$  radio luminosity - calculated based on NVSS integrated flux density - for all FR II quasars identified in our sample plus all FR II sources with  $z \leq 0.7$  from deVries et al. (2006).

source reveals: a) NVSS measures are larger than corresponding FIRST values for virtually all FR II sources and b) most CD RL sources show agreement between FIRST and NVSS measures with a scatter of  $\sim \pm 20 \text{ mJy}$ , most likely due to variability (see also Wang et al. 2006). In a few extreme cases we see differences of up to  $\sim \pm 300 \text{ mJy}$ . There is no evidence for a significant population of CD RL sources with excess NVSS flux density that might be due to extended structure not seen by FIRST.

We found  $n=48$  FR IIs brighter than psf  $g=17.5$  OR psf  $i=17.5$ . NVSS flux density measures were always preferred over FIRST (for all sources, not only for FR IIs). The small size of the FR II sample motivated us to add double-lobe quasars in our redshift range that were identified by deVries et al. (2006) based on DR3. Careful reexamination of optical spectra and radio maps for this addition caused us to eliminate several objects (e.g. no broad emission lines, no FR II morphology, no radio detection). The DR3-based sample, which added  $n=67$  FR IIs, was not optically constrained, and most of the quasars in that subsample showed apparent magnitudes fainter than our g or i-band limits. Their sample is not meant as an exhaustive list, but the search algorithm had a reported accuracy of  $\sim 98\%$  for identifying FR II sources.

Figure 2 shows the radio luminosity distribution for the  $48+67=115$  FR II sources. The weakest bona fide FR II/quasar found shows  $\log L_{1.4GHz} = 31.6 \text{ (erg s}^{-1} \text{ Hz}^{-1})$ . Thus, this becomes our radio-luminosity defined boundary between RL and RQ QSOs (Criterion 1). The FR II sources in this sample span three orders of

**Table 2.** Additional samples with  $z < 0.7$  used in this study, but not measured spectroscopically. We require that they all show bona-fide Type 1 QSO spectra.

Apparent Magnitude	Category/Type	$N_{total}$	$N_{radio-detected}$	$N_{RL}$
psf $g < 17.5$	“Galaxy”-labeled by SDSS	16	12	0
psf $i < 17.5$ AND psf $g \geq 17.5$	“Galaxy”-labeled by SDSS	81	33	1
psf $g \geq 17.5$ AND psf $i \geq 17.5$	double-lobed (FRII) from deVries et al. (2006)	67	67	67
$19.0 \leq \text{psf } g < 19.5$	“QSO”-labeled by SDSS	4800+	134	47
$19.0 \leq \text{psf } i < 19.5$	“QSO”-labeled by SDSS	3800+	80	31

Notes: For the last two samples listed in the table one can notice the very large  $N_{total}$  and a very small  $N_{radio-detected}$ . We required a SDSS/FIRST optical match within one arcsec. We are not concerned about completeness of these subsamples used in § 5 and § 6. Our sample already included all sources from deVries et al. (2006) that have psf  $g < 17.5$  OR psf  $i < 17.5$ .

magnitude in radio luminosity (median  $\log L_{1.4GHz} = 32.9 \text{ erg s}^{-1} \text{ Hz}^{-1}$ ), although they become relatively rare above  $\log L_{1.4GHz} \sim 33.5 \text{ erg s}^{-1} \text{ Hz}^{-1}$ . Figure 2 shows a continuous distribution of radio powers, with a clear decline in the number of sources toward our RL/RQ nominal boundary. The shape of the distribution suggests that there could be only a very small number of FRIIs weaker than our weakest bona-fide FRII quasar. It is beyond the scope of the paper to fully examine the true nature of the functional form describing the FRII radio-luminosity distribution. However, we attempted a comparison with the dual population model for the radio-luminosity function proposed by Willott et al. (2001) for steep spectrum radio sources. We extrapolated the 1.4GHz measures to 151 MHz measures (to allow for common grounds with that study) two ways: 1) assuming a spectral slope  $\alpha_\nu$  of 0.5 and 2) using the empirical scaling relation suggested by K rding et al. (2008) (their equation (5)). Either way, we do not see a decline on the lower luminosity side as abrupt as presented in Figure 3 of Willott et al. (2001). Secondly, the  $L_{151MHz}$  distribution that we get peaks about one decade fainter ( $\sim 25.5 \text{ W Hz}^{-1} \text{ sr}^{-1}$ ) than their model suggests for high luminosity population alone (although their low-luminosity population could also include FRII sources). While not complete, the sample we explore is large enough to be assumed representative of the FRII RL phenomenon in broad line emitting quasars within  $z = 0.7$ .

A recent study (Lu et al. 2007) reported eleven extended SDSS radio quasars weaker than  $\log L_{1.4GHz} \sim 31.5 \text{ erg s}^{-1} \text{ Hz}^{-1}$  (see their Figure 2). The authors kindly provided us the list of those sources and we analyzed them one-by-one. Two of them are included among our RI and are also listed in Table 3 (SDSS J110717.77+080438.2 and SDSS J120014.08-004638.7). One other source is also in our sample as RQ with  $\log L_{1.4GHz} = 30.7 \text{ erg s}^{-1} \text{ Hz}^{-1}$  (SDSS J162607.24+335915.2). All other sources are unambiguously RQ, in some cases offset a few arcseconds from the optical quasar and were assumed in Lu et al. (2007) to be associated with the active nucleus.

The goal of our work was to search for a dichotomy or gap in radio properties between RQ and RL sources. Of course, sources are found with radio intermediate properties (e.g. Falcke et al. 1996a; Sulentic et al. 2003). Another goal of this paper was to isolate a population of these radio-intermediate (RI) sources and try to determine if they form a unique (special) class of quasars. Unlike the non-RL/RL boundary we have no clear empirical basis for defining a RQ/RI boundary because all RI show CD radio morphology. The best that we can do is to isolate a region that is most clearly RI. Considering that: a) at our sample redshift limit ( $z=0.7$ ) the minimum detectable radio luminosity (within FIRST/NVSS) is  $\log L_{1.4GHz} \simeq 31.0 \text{ erg s}^{-1} \text{ Hz}^{-1}$  and b) the radio-FIR (Far Infrared) correlation spans over five decades in luminosity and extends up to  $\log L_{1.4GHz} \simeq 31.0 \text{ erg s}^{-1} \text{ Hz}^{-1}$  (e.g.

Condon 1992; Yun et al. 2001), we see that value as a reasonable boundary between star-formation and AGN-dominated radio activity (Sopp & Alexander 1991, Kukula et al. 1998 and Haas et al. 2003 show that RQ QSOs follow the radio-FIR correlation). We therefore define RI sources as those with  $\log L_{1.4GHz}$  in the interval  $31.0\text{--}31.6 \text{ erg s}^{-1} \text{ Hz}^{-1}$ . This is a much more restricted RI definition than the one given in Falcke et al. (1996a).

In brief, a source is considered RL if its  $L_{1.4GHz}$  radio power is at least  $31.6 \text{ erg s}^{-1} \text{ Hz}^{-1}$ . A source is considered RI if its  $L_{1.4GHz}$  radio power is at least  $31.0 \text{ erg s}^{-1} \text{ Hz}^{-1}$ , but less than  $31.6 \text{ erg s}^{-1} \text{ Hz}^{-1}$ . All other sources are RQ.

Summarizing, we considered the whole sample obtained from the combination of psf  $g < 17.5$ , psf  $i < 17.5$  with an “OR” logical operator. The total number of sources was  $N=1770$  ( $n=95$  RL). The sample adopted for spectroscopic evaluation (see Table 1) is constructed as follows:

- (i) all RL and RI QSOs that are brighter than either psf  $g = 17.5$  or psf  $i = 17.5$ ;
- (ii) all RQ QSOs (radio-detected or undetected) that are brighter than psf  $g = 17.0$  and
- (iii) all RQ QSOs that are radio detected and show psf  $g$  in the range  $17.0 - 17.5$ .

We visually examined the SDSS spectrum for every source and rejected objects without emission lines (e.g. SDSS J075445.67+482350.7), objects without broad lines (e.g. SDSS J103900.37+414008.7, SDSS J104451.72+063548.6) or with bad pixels (e.g. SDSS J113109.49+311405.5, SDSS J145638.81+442755.2, SDSS J220103.13-005300.2) that prevented reliable line measures in the region of interest. We rejected one supernova: SDSS J113323.97+550415.8 - as reported by Zhou et al. 2006. Two FRII quasars (SDSS J092414.70+030900.8 and SDSS J123915.39+531414.6) showed serious host galaxy contamination (psf  $g - \text{psf } i > 1.0$  in both cases), the broad component of  $H\beta$  could not be measured. We also excluded from our analysis objects with  $W(H\beta) \leq 20\text{\AA}$ , which can be sources in a high continuum phase (e.g. SDSS J150324.77+475829.6) and/or very red continua with extreme Balmer decrement, where  $H\alpha$  is completely different from  $H\beta$  (e.g. SDSS J004508.65+152542.0).

We should emphasize that our spectroscopic analysis does not include rare objects with extreme  $R_{FeII} > 2.0$  values. Sources with extremely strong FeII tend to be very red ( $u-g > 0.8$ ), strong IR emitters (Lipari et al. 1993; for a detailed study of such a case see V eron-Cetty et al. 2006) and are not suitable for the FeII template adopted for this study. We identified three RL sources whose spectra show extreme FeII emission ( $R_{FeII}$  much larger than 2.0): SDSS J094927.67+314110.0, SDSS J144733.05+345506.7, SDSS J152350.42+391405.2. Our attempt to fit the IZw1-based (Boroson & Green 1992) template for such objects was unsuccessful.

ful, thus they are not shown in Figure 4. Such objects require special attention and is beyond the purpose of the present study to focus on their nature. The inclusion of such pathological and relatively rare cases will not affect the conclusions of the present study. We were able to make reliable measures in the  $H\beta$  region for  $N=477$  objects. Our RL/RI sample is complete to 17.5 apparent magnitude in g- OR i-band. We are confident that the RL+RI sample is at least 75% radio-complete because all have a FIRST  $S(1.4\text{GHz}) \geq 1.5$  mJy (see Figure 1 of Jiang et al. 2007). Our RL sample includes  $n=85$  RL quasars ( $n=46$  FRII) and  $n=59$  RI QSOs. The remaining  $n=333$  represent our RQ sample which, while incomplete, is large enough to be representative for the RQ parent population. Our final sample includes sources spanning the extinction corrected i-band range  $-27.5 \leq M_i \leq -17.1$ . We cross-checked our entire sample selected based on  $\text{psf } g < 17.5$  (806 “QSO” + 16 “Galaxy” - see Tables 1 and 2) with the “vetted” QSO catalog Schneider et al. (2007). All sources in our sample with  $M_i$  brighter than  $-22.0$  are present in the that catalog. All sources in that catalog satisfying our selection criteria are found in our sample. No additional QSO satisfying our selection criteria was found there.

### 3 ANALYSIS OF OPTICAL SPECTRA FROM SDSS

In order to obtain the optical parameters of the 4DE1 we followed the analysis procedure described in Marziani et al. (2003a)<sup>6</sup>. An underlying power-law  $f_\lambda \sim \lambda^\alpha$  continuum was defined using regions minimally contaminated by FeII lines, specifically at 4195-4215 Å and 5700-5800 Å; it was decided prior to fitting the FeII template. We used the IZw1-based template of Boroson & Green (1992) for FeII decontamination. This represents an important advantage over our own Atlas sample (Marziani et al. 2003a) where the typical wavelength coverage of the spectra was  $\sim 1000\text{\AA}$ , rendering continuum estimation very uncertain. Our chief goals from FeII template fitting are: 1) to obtain  $W(\text{FeII } 4750\text{\AA})$  blend and 2) to clean up the  $H\beta$  region.

In about 20% of sources we attempted to remove the host galaxy contamination<sup>7</sup> before deriving 4DE1 parameters using the library of theoretical galaxy templates from GALAXEV<sup>8</sup> of Bruzual & Charlot (2003). A much more sophisticated approach is proposed by Zhou et al. (2006). All our sources with noticeable host galaxy contamination lie within  $z=0.2$ . There seems to be an apparent contradiction with the results of Vanden Berk et al. (2006). They use an eigenspectrum decomposition technique and report a non-zero host galaxy contamination all the way to  $z=0.7$ . Our sole purpose was to clean up the spectral region of interest of the most prominent absorption lines of a host galaxy. We make no attempt to estimate the relative proportion of AGN and host light in the spectrum unless clear absorption lines are observable; the spectra have good S/N to reveal potential host contaminations. Evidently, most objects we deal with tend to have bluer continua (see Figure 1 and the previous section that explains how we built-up our sample) and thus are less affected by host galaxy. It is possible that

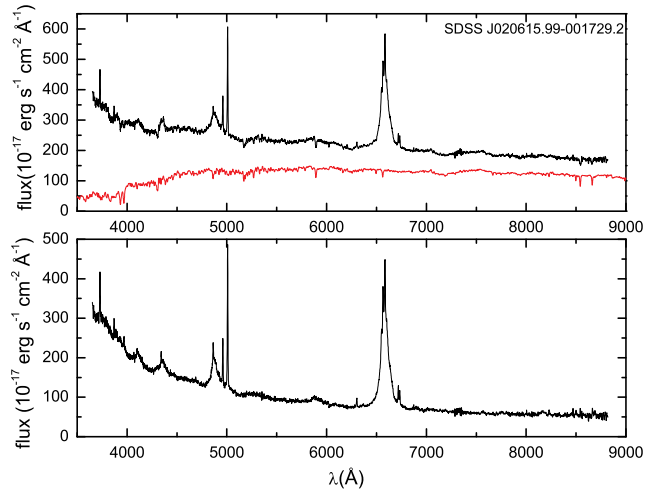


**Figure 3.** An example of a QSO contaminated spectrum. The top panel shows the initial SDSS spectrum (black) and a template of a host galaxy (red); the bottom panel shows the QSO spectrum after subtracting the spectrum of the host galaxy.

many of the RQ sources not considered for our spectroscopic reduction have a significant host galaxy contribution at redshifts higher than 0.18. We are also aware that we severely under-represent the population of low  $z$  objects that form the “bump” in Figure 1. As we try to explain in this section, the FWHM  $H\beta$  seems to be minimally responsive to this uncertainty in the relative amount of flux from a host galaxy. See Figure 3 for an example of the host galaxy “removal”. In most cases this process turned out to be very effective in revealing the QSO emission line spectra. We tested the effect of host galaxy subtraction on our spectroscopic measures and found that  $\sim 60\%$  of these sources (that required this step) were seriously contaminated and the rest moderately/weakly contaminated. For the latter, we attempted an estimate of the 4DE1 optical plane both before and after the correction. We found that FWHM  $H\beta$  changes randomly within  $\pm 5\%$ , but  $R_{FeII}$  was much more sensitive to this procedure, with a 25-35% systematic change toward lower  $R_{FeII}$  values. Our set of contaminated spectra span a wide range of 4DE1 parameters values.

When clear inflections were observed between the broad and narrow components of  $H\beta$ , we did not constrain the width of the latter component to be the same as FWHM  $[\text{OIII}]\lambda\lambda 4960, 5008\text{\AA}$ . No attempt was made to decompose the broad Balmer line into components. A spline function was used to fit its global profile.

We compare the values obtained in the present study for FWHM  $H\beta$  and  $R_{FeII}$  with those measured in Marziani et al. (2003a) for the  $n=38$  sources in common with that Atlas. We calculated  $\Delta\text{FWHM } H\beta$  and  $\Delta R_{FeII}$  for every object (of these 38) considering in each case the values obtained in the current study and those in the Atlas (2003). The mean and median differences are a reasonable indicator of the robustness of the 4DE1 parameter space in its optical dimensions. We find a scatter of  $\sim 10\text{-}20\%$  for FWHM  $H\beta$  (no systematic effect) and for  $R_{FeII}$  we report a systematic effect of 30-35% toward larger values in our present study. This latter effect may be due to a more reliable choice of the continuum and/or a higher quality of spectral signal. For Figures 4 and 5 we conservatively adopt the uncertainties estimated in the Atlas (2003), even though the quality of the spectra is clearly better in our present sample. We are aware that the  $R_{FeII}$  gap (c.f. Figure 4) between 0 and 0.1 is not physical and most likely reflects the

<sup>6</sup> We used Image Reduction and Analysis Facility (IRAF), distributed by the National Optical Astronomy Observatories, which are operated by the Association of Universities for Research in Astronomy, Inc., under cooperative agreement with the National Science Foundation - <http://iraf.noao.edu/>

<sup>7</sup> When prominent absorptions lines like Mg  $\lambda 5177\text{\AA}$  and Na  $\lambda 5896\text{\AA}$  are present

<sup>8</sup> <http://www.cida.vc/~bruzual/bc2003>



difficulty of measuring very low values of  $W(\text{FeII } \lambda 4570\text{\AA})$ . Such an effect could be due at least in part to our simple definition of the optical continuum. We would like to explore more on this issue in a future project.

#### 4 LOCUS OF RL AND RI QUASARS IN THE 4DE1 OPTICAL PLANE

The optical plane of 4DE1 provides a powerful diagnostic tool for testing whether the RL and non-RL sources are spectroscopically different. We earlier proposed the existence of two QSO populations A and B separated at  $\text{FWHM } H\beta \simeq 4000 \text{ km s}^{-1}$  (see the Introduction and section 3.2 of Sulentic et al. 2007; see also section 3 of Sulentic et al. 2000a).

The previously reported restricted domain occupation of RL sources in 4DE1 space means that we can now ask if: 1) the SDSS sample confirms the earlier restricted RL domain occupation and 2) if RI sources show domain occupation more similar to RL or RQ Type 1 AGN. Figure 4 shows the distribution of RL and non-RL sources in the optical plane of 4DE1 (non-RL include  $n=333$  RQ +  $n=59$  RI). Figure 4 clearly confirms a restricted domain space occupation for RL sources with  $\sim 78\%$  falling above  $\text{FWHM } H\beta=4000 \text{ km s}^{-1}$  (our so-called population B domain: Sulentic et al. 2000a); 91% of FRIIs and 62% of CD RL quasars are in this Population B. The horizontal line in Figures 4 and 5 marks this nominal populations boundary. RQ QSOs show a much wider domain space occupation with more than half ( $\sim 62\%$  of our sample) lying below  $\text{FWHM } H\beta=4000 \text{ km s}^{-1}$ . If 4DE1 parameters measure aspects of Broad Line Region (BLR) kinematics and geometry then this domain occupation difference is consistent with a physical difference between RL and the majority of RQ sources, which supports a RQ-RL bimodality. At the very least past work reported that RL sources show systematically higher black hole masses and systematically lower Eddington ratios than the RQ majority (e.g. Marziani et al. 2001; Boroson 2002; Marziani et al. 2003b; Sulentic et al. 2006).

We performed a 2D Kolmogorov-Smirnov (K-S) test in order to evaluate the significance of: 1) the RQ-RL difference and 2) the RL FRIIs - RL CDs difference in domain occupation. Following the routine available in Numerical Recipes<sup>9</sup> the K-S procedure (Peacock 1983; Fasano & Franceschini 1987) divides the optical plane into quadrants that maximize the two population difference. For test 1) the RQ sample is assumed to represent the parent Type 1 AGN population and RL the test sample. For test 2) the RL FRII sample is assumed to represent the parent population and the RL CDs the test sample. The results of the two tests are summarized in Table 3. One can notice that the RL/non-RL separation at  $\text{FWHM } H\beta = 3875 \text{ km s}^{-1}$  is in reasonable agreement with our previously adopted Population A/B boundary at  $4000 \text{ km s}^{-1}$  (Figure 4). As reported in Table 3, the probability that RL and RQ occupy the same spectroscopic domain is very low. Similarly, the second test between FRIIs and RL CDs shows that the two samples are very distinct in terms of spectroscopic properties. In the former case the result is equivalent to saying that it is extremely unlikely that RL and non-RL are drawn from the same parent population. In the later test, the probability listed in Table 3 could be interpreted in two ways: 1) the orientation is responsible for the distinct space occupation for FRIIs and RL CDs or 2) the CD RLs and the FRIIs are drawn from distinct populations, in which case the RL CDs (all

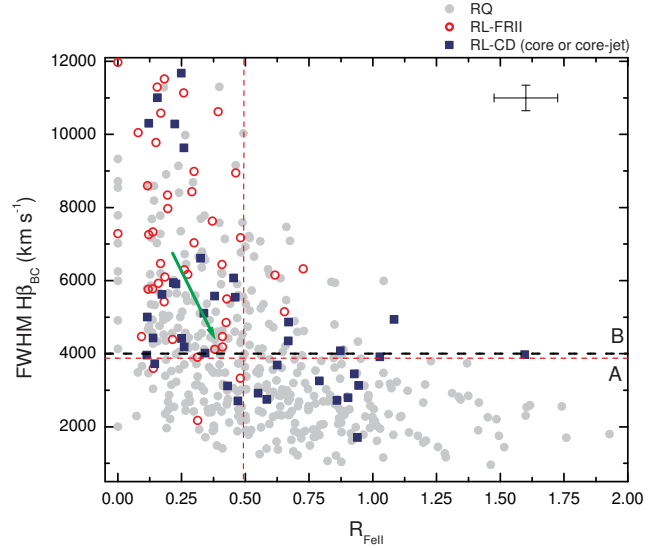


**Figure 4.** RL quasars in the optical plane of the 4DE1 parameter space. The green arrow indicates the displacement between the median  $\text{FWHM } H\beta$  and the median  $R_{\text{FeII}}$  for the FRII and the CD sources. The solid light gray symbols are non-RL objects. In the upper right corner are indicated the typical  $2\sigma$  errors, estimated in Marziani et al. (2003a). The red dotted lines show the boundaries for the quadrants defined by the 2D K-S test we performed as we explained in the text. The black dotted line indicates the Population A/B boundary. The vertical axis is truncated at  $12000 \text{ km s}^{-1}$  for clarity, thus we miss showing five other RL (two CD and three FRIIs between  $12000$ - $24000 \text{ km s}^{-1}$ ).

or most of them) could be interpreted either as beamed RQs or as pre-/postcursors of an FRII episode.

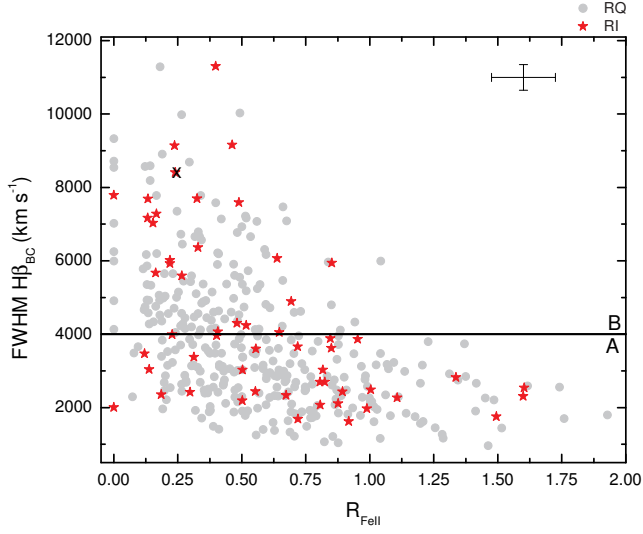
There is also a clear bimodality of RL/RQ in terms of  $R_{\text{FeII}}$  (robustly confirmed by the 2D K-S test we performed). In the context of 4DE1 we focus on  $\text{FWHM } H\beta$  for several reasons: 1) it is a direct measure of the Broad Line Region (BLR) kinematics, 2) it can be measured more accurately than  $R_{\text{FeII}}$  (see § 3) and 3) there are significant Population A/B differences reported over the last seven years that are defined in terms of  $\text{FWHM } H\beta$  alone (see Table 5 in Sulentic et al. 2007).

Figure 4 then shows a significant displacement between the non-RL and RL distributions with most RL lying above  $\text{FWHM } H\beta=4000 \text{ km s}^{-1}$ . We also observe a separation between the mean/median position of FRII RL sources and core/core-jet (CD) RL sources (see Table 4), confirming a result from Sulentic et al. (2003). This is the first step in estimating the role of source orientation in 4DE1. The vector shown in Figure 4 indicates the change in median 4DE1 optical parameters between FRII and CD RL sources. Orientation-unification scenarios see the latter sources as having radio jets aligned to within a few degrees of our line of sight. The vector suggests that source orientation strongly influences  $\text{FWHM } H\beta$  measures and, to a lesser degree,  $R_{\text{FeII}}$ . Given the likelihood that large disk-jet misalignments can occur and that radio structure in many RL is highly nonlinear it is surprising how large is the FRII-CD median parameter separation. The 10-20% of CD and FRII RL with, respectively, very large and very small  $\text{FWHM}$  values could be interpreted as sources where the radio structure and the region that emits the broad lines (i.e. accretion disk) appear to be misaligned, if one invokes the unified picture for AGNs relative to Figure 4. The few RL CDs with very large  $\text{FWHM } H\beta$  may, apparently disconnected from the bulk of RL CDs, may be the best candidates for a pre- or post- FRII phase. Sources with

<sup>9</sup> www.nr.com

**Table 3.** Two-dimensional Kolmogorov-Smirnov tests for RL / non-RL and for RL FRII / RL CD.

Samples n1-parent and n2-test	Coordinates of quadrants FWHM $H\beta$ ( $\text{km s}^{-1}$ ) ; $R_{FeII}$	Probability of null hypothesis
392-non-RL and 85-RL	3875 ; 0.49	$P \sim 6.2 \times 10^{-8}$
46-RL FRII and 39-RL CD	6100 ; 0.18	$P \sim 9.8 \times 10^{-4}$

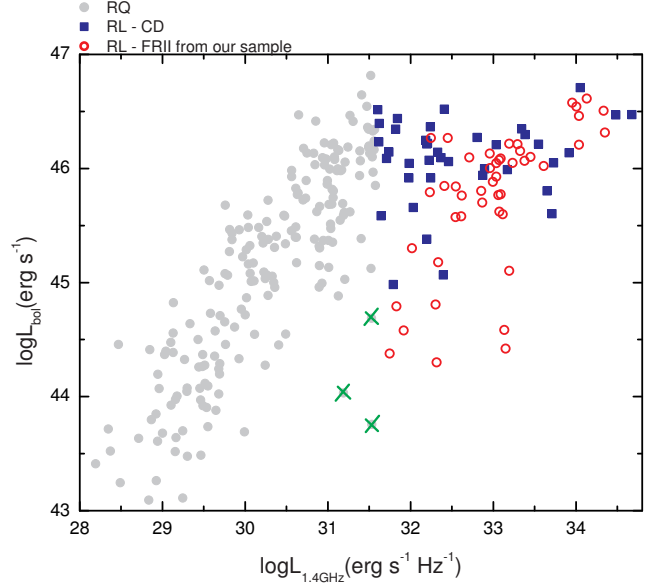
**Figure 5.** RI QSO in the optical plane of the 4DE1 parameter space. The light gray symbols show the RQ objects and the solid red stars are the  $n=59$  RI sources. SDSS J232721.97+152437.3 is indicated with an “X” - see “Discussion” and also Table 3. The vertical axis is truncated at 12000  $\text{km s}^{-1}$  for clarity, thus we miss showing two other RI.

extremely broad Balmer profiles (sometimes double peaked) are so rare (we find a handful of such sources with FWHM  $H\beta$  in the range 12000 - 30000  $\text{km s}^{-1}$ ) as to defy interpretation as the simple tail of a normal QSO FWHM distribution.

Figure 4 included RI along with the RQ QSOs as non-RL QSOs. The tacit assumption was that RI and RQ are the same. Figure 5 presents a test of that assumption that is equivalent to that performed for RL. Does the previously defined RI sample show a distribution in the optical plane of 4DE1 more similar to RL or RQ sources? The  $n=59$  RI sources (stars in Figure 5) show no distinguishable difference in occupation from the  $n=333$  RQ sample. Only 42% of the RI population is found in the Population B domain, comparable to the  $\sim 37\%$  for the RQ sources. There is therefore no spectroscopic evidence that the RI sources form a special class (see Table 4).

## 5 CAN WE REVEAL A RL/RQ DICHOTOMY USING L-DEPENDENT DIAGRAMS?

The previous section compared RQ, RL and RI sources in a Luminosity-independent context. We now address the problem of a RL/RQ dichotomy from a Luminosity-dependent perspective. Figure 6 plots source bolometric versus radio luminosity ( $L_{bol}$  vs.  $L_{1.4GHz}$ ). The radio luminosity is K-corrected (Hogg 1999) assuming that  $f_\nu \sim \nu^\alpha$  and  $\alpha = -0.5$  in the radio regime. The bolometric luminosity was estimated from  $L_{bol} \simeq 10\lambda L_\lambda$ , where  $\lambda \equiv 5400\text{\AA}$  (see a concise discussion on the bolometric correction in section 2.8

**Figure 6.** The distribution of our relatively bright sources in a plane defined by the bolometric and radio luminosity. The three objects marked with an X are commented in Table 3 and related discussion in § § 8.1. The radio-undetected QSOs are not shown here.

of Marziani et al. 2006, and references therein). The 5400 $\text{\AA}$  specific luminosity is estimated using the continuum flux in the rest-frame spectrum of the QSO. We used *dopcor* task in IRAF with the the appropriate cosmological flux corrections applied when deredshifting the spectra. Our sample covers about four decades in bolometric luminosity with  $\log L_{bol} \sim 43.0-47.0 \text{ erg s}^{-1}$ .

There are a few important comments about Figure 6: a) we find no RL quasar fainter than  $\log L_{bol} = 44.3 \text{ erg s}^{-1}$ , b) we find no CD RL below  $\log L_{bol} \simeq 45.0 \text{ erg s}^{-1}$ , c) the RQ sample shows a power-law correlation ( $L_{bol} \propto L_{1.4GHz}^{0.89}$ ) (see also e.g. Kukula et al. 1998) or alternatively  $L_{1.4GHz} \propto L_{bol}^{0.85}$  (the same as reported in White et al. 2007, considering that  $L_{bol} \propto L_{opt}$ ) but d) the RL population however shows a different behavior for CDs and FRIIs. The majority of CDs concentrate at high values of  $L_{bol}$ , while the distribution of FRII quasars shows a rough correlation parallel to the RQ one. Most of the CDs, especially below  $\log L_{1.4GHz} \simeq 32.5$ , make no sense in an orientation unification scenario because there is no corresponding weaker FRII population to the left of them from which they could be boosted. As we suggested in § 4 based on the 2D K-S test for FRIIs/RL CDs these sources could be seen as boosted RQs.

4DE1 parameters show no obvious dependence on source luminosity. They also show no dependence on radio luminosity apart from a restricted domain space occupation observed only for RL sources. If RQ and RL sources belong to the same family then we could reasonably expect them to follow the same correlation



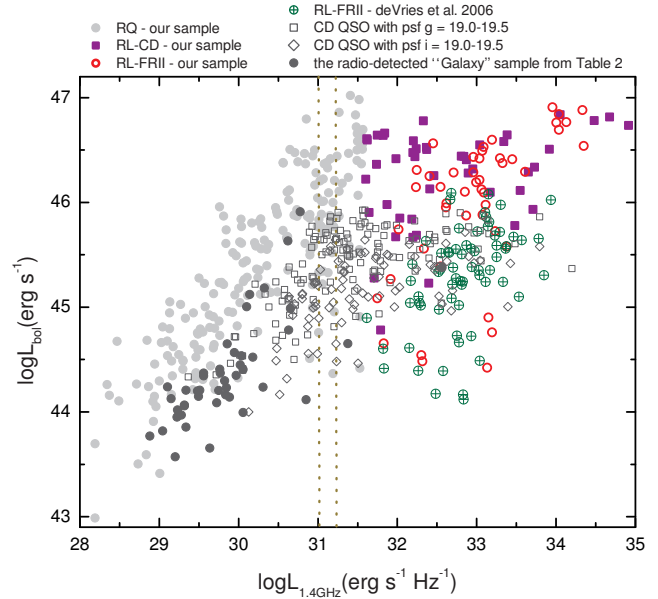
**Table 4.** Mean and Median optical spectroscopic measures for the samples used in Figures 4 and 5.

	mean±standard deviation		median	
	FWHM H $\beta$ (km s $^{-1}$ )	R $_{FeII}$	FWHM H $\beta$ (km s $^{-1}$ )	R $_{FeII}$
Relative to Figure 4				
RL (n=85)	6809±3976	0.36±0.29	5775	0.27
non-RL (n=392 RQ+RI)	4016±2569	0.57±0.38	3375	0.50
RL FRII (n=46)	7673±3733	0.26±0.17	6750	0.20
RL CD (n=39)	5789±4059	0.48±0.36	4418	0.38
Relative to Figure 5				
RQ (n=333)	3852±2114	0.56±0.35	3227	0.50
RI (n=59)	4941±4230	0.62±0.52	3659	0.50

between bolometric and radio luminosity. Figure 6 suggests that RQ and RL sources show separate correlations. We see a clear *dichotomy* between the populations at our previously determined boundary ( $\log L_{1.4GHz} = 31.6 \text{ erg s}^{-1} \text{ Hz}^{-1}$ ) as lower limit for RL activity. This dichotomy appears to independently confirm our previous suggestion, based on 4DE1 occupation, that RQ and RL sources are fundamentally different.

Figure 6 is based upon our bright SDSS sample. Does it include all FRII quasars within  $z=0.7$ ? What is the effect on Figure 6 of including fainter sources in the same redshift range? Consideration of these questions can help us understand why such conflicting results about a RQ-RL dichotomy/bimodality have been obtained in past studies. We have reason to fear that Figure 6 does not tell the full story about dichotomy because almost all sources in our sample with  $\log L_{bol} < 45.5 \text{ erg s}^{-1}$  show  $z \leq 0.15$  while all sources above that value show  $z > 0.15$  (see Figure 8). We have essentially sampled the bright end of the low redshift Optical Luminosity Function (OLF). On this bright end RL sources are relatively abundant and RQ numbers small enough to allow a dichotomy to be seen. But we have severely undersampled the faint end of the OLF (e.g. Boyle et al. 2000; Croom et al. 2004; Richards et al. 2005, 2006). In that luminosity range the RQ population is so large that the radio bright tail of the RQ distribution might overlap the RL distribution effectively quenching any dichotomy.

The above suggestion can be tested and illustrated by adding fainter subsamples of QSOs (see Table 2) to Figure 6, leading to Figure 7, which shows the following : i) the  $n=67$  sample of FRII from deVries et al. (2006), fainter than our sample of FRII (see § 2); ii) all radio-detected objects that are labeled “Galaxy” by the SDSS spectro-pipeline but show Type 1 spectra (no spectroscopic reduction was performed on these, as we explained earlier); iii) core radio sources (no FRIIs) with psf  $g$  in the range 19.0-19.5 and iv) core radio sources (no FRIIs) with psf  $i$  in the range 19.0-19.5. In order to understand some of the subtle effects that come into play at this point Figure 7 should be approached in conjunction with Figures 8 and 9. We point out that for Figures 7 and 8 we estimated the bolometric luminosity following the empirical results of Hopkins et al. (2007) - first estimating the B-band luminosity for our sources obtained from psf  $u$  and psf  $g$  magnitudes (corrected for extinction, using the SDSS coefficients). The B-band luminosity (K-corrected, assuming that  $f_\nu \sim \nu^\alpha$ , where  $\alpha = -0.5$  in the optical domain) was obtained from psf  $u$  and psf  $g$  magnitudes using the transformation formula proposed by Jester et al. (2005a). We make

**Figure 7.** The distribution of our relatively bright sources plus several subsamples of QSOs selected as explained in the text. The radio-undetected QSOs are not shown here. The vertical dotted lines at 31.0 and 31.2 represent the minimum detectable radio luminosity that corresponds to a detection limit of 0.7 - 1.0 mJy at  $z=0.7$ , respectively.

no attempt to reduce the spectra of these faint objects and therefore no 5400Å specific luminosity (in the underlying continuum) can be estimated and used to estimate  $L_{bol}$ . This is why we employ the the empirical recipe from Hopkins et al. (2007). It is worth mentioning that we examined every optical spectrum and radio image in FIRST/NVSS to confirm Type 1 optical and FRII/CD radio status. No attempt was made to estimate a host galaxy contribution for these fainter sources. The main results of this study (e.g. Figures 6, 7 and 8) are not sensitive to the choice of the bolometric correction. We also remind the reader that the distribution in Figure 9 reflects the heterogeneous construction of the radio sample we investigated, as explained in the previous sections.

In Figure 7 it is now obvious that the optically faint radio core sources (the empty squares and diamonds) tend to fill in the region  $\log L_{bol} \sim 44.0 - 46.0$  and  $\log L_{1.4GHz} \sim 30.5 - 32.0$ . The fact that such objects are less luminous than  $\log L_{bol} = 46.0$  is not a surprise.

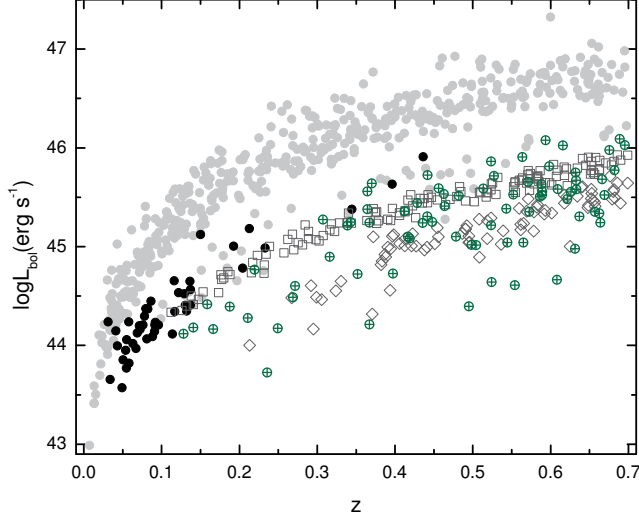


**Figure 8.** The luminosity distribution with redshift for the various subsamples of QSOs employed in Figure 7; the symbols are similar to those in Figure 7, with the exception that this time all QSOs in our sample (RQ, RL CDs and RL FRIIs) are displayed with the same solid light grey symbols. The crossed-circles denote only the FRII subsample from deVries et al. (2006), just as in Figure 7.

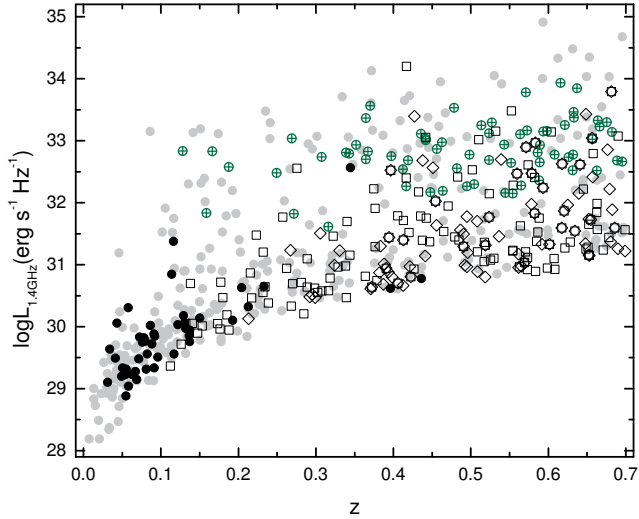


**Figure 9.** The radio luminosity distribution with redshift for the various subsamples of QSOs employed in Figure 7 and 8; the symbols are identical to those in Figure 8.

They are selected as apparently fainter objects in the same  $z$  range as the bright sample. It is important noting that these fainter samples (iii and iv above) are not represented below  $z=0.1$  and  $z=0.2$ , respectively. This is the main cause of their tendency to scatter mostly in the region that was previously (in Figure 6) scarcely populated along the radio-luminosity axis. The main conclusion we get is that the picture of the dichotomy becomes “blurry” at this point.

With the addition of the fainter FRIIs from deVries et al. (2006) we observe the parallel RL FRII sequence more clearly in Figure 7. The trend we see for FRII quasars is qualitatively similar to that reported by other studies for steep-spectrum quasars using lower radio frequencies (e.g. Serjeant et al. 1998; Willott et al. 1998) or higher radio frequencies (Xu et al. 1999). The two correla-

tions likely indicate a different fraction of power output channeled into the jets (e.g. Rawlings & Saunders 1991; Miller et al. 1993). The core of RL population covers  $\sim 2.5$  dex in the  $L_{bol}$  space and  $\sim 2$  dex in the  $L_{1.4GHz}$  space, while the RQ sample distributes over  $\sim 4$  dex in either measure. The small number of extreme sources above  $\log L_{bol} \sim 46.5$  lie near our high redshift limit and suggest that we are seeing the first hints of luminosity evolution in our sample.

## 6 ESTIMATING THE RADIO LOUD FRACTION (RLF) OF TYPE 1 AGN

We are now in a position to estimate the fraction Radio Loud quasars relative to the total population of QSOs that satisfies our redshift and luminosity criteria. Figure 1 shows that an  $i$ -band selection adds a large number of relatively low redshift sources. Blue ( $g$ -band) selection provides a more uniform sampling of sources in our redshift range. If we consider only sources with  $psf\ g < 17.5$  the RLF  $\simeq 9.2\%$  (of  $n \sim 822$  sources, i.e. 806 QSO + 16 “Galaxy” - see Tables 1 and 2). Considering sources selected with  $psf\ i < 17.5$  yields a RLF  $\simeq 5.2\%$  (relative to  $n \sim 1737$  objects, i.e. 1656 “QSO” + 81 “Galaxy” - see Tables 1 and 2). If we combine the above conditions with a logical “OR” operator we get RLF  $\simeq 5.4\%$ , relative to  $n \sim 1770$  objects.

Our results are quite different compared to the RLF estimate for the PG sample of QSOs; RLF  $\sim 17\%$  (applying our definition of radio-loudness to the sample of 87 sources in Boroson & Green 1992 or directly to the full list of 96 Palomar-Green UV-excess selected QSOs/Seyferts from Green et al. 1986 with  $z < 0.5$ ). Boroson & Green (1992) include 50 Population A sources (two of them RL) and 37 Population B sources (twelve of them RL). Obviously, one must also bear in mind that the absolute magnitude cut at  $M_B = -23$  in the PG sample (Boroson & Green 1992) has its play into the rather large RLF it includes, considering also our results presented in Figure 6; we find no RL in the dimmest decade of bolometric luminosity we sampled. This is also consistent with the reported dependence of RLF on luminosity (see the “Introduction” for references related to this issue).

Jester et al. (2005a) offered a detailed discussion on possible radio-related incompleteness in the Palomar-Green Bright Quasar Survey (Schmidt & Green 1983; Green et al. 1986) compared to an  $i$ -band limited sample from the SDSS. They suggest that the rather large RLF in the BQS appears connected to the fact that BQS objects, being selected in a  $B$ -band flux-limited survey, have rather blue continua, objects with bluer continua apparently tend to have stronger [OIII] lines, and objects with larger [OIII] lines are more likely to be radio-loud. In the present study we also find a RLF fraction approximately double when selecting the sample based on a bluer filter ( $g$ -band) than when selecting based on a redder one ( $i$ -band). On the other hand Jester et al. (2005a) find no systematic radio-related biases by comparing the BQS sample against a BQS-like sample selected from SDSS database. More recently, two other SDSS/FIRST - based studies (deVries et al. 2006; Lu et al. 2007) found that FRII quasars are rather bluer than the radio-compact sources, which apparently could be connected to the RL excess in BQS survey. Indirectly confirming their conclusion (i.e. corroborated with our results that the large majority of FRIIs are members of Population B) is the study of Richards et al. (2003), which report a systematic narrowing of the  $H\beta$  line with increasing redness.

However, the cause of the RL excess in PG survey is not completely clear at this time, considering also the apparently contradictory conclusions about the optical colors of radio quasars, i.e.

RL quasars have been found to be in general redder than RQ QSOs (e.g. Brotherton et al. 2001; Ivezić et al. 2002; White et al. 2007; Labita et al. 2007).

## 7 4DE1 OPTICAL PLANE AND THE RADIO-LOUDNESS PROBABILITY

4DE1 is a diagnostic tool that could set empirical constraints for the theoretical models of AGN physics. Our results show that RL quasars prefer a restricted zone of occupation in the optical plane of 4DE1 (Figure 4). Our g-band selected sample of  $n=333$  QSOs ( $n=34$  RL) is the most complete that we have available for this analysis. The fractions of Population A and B sources are  $\sim 60\%$  and  $\sim 40\%$  respectively of which 4-5% and 17% are RL. The situation is even more extreme if we correct sources for line-of-sight orientation (see Figure 4). In an orientation unification scenario many of the Population A RLs (mostly CDs) could simply be face-on oriented Population B RLs. FRII sources can be said to define the locus of the RL population in the 4DE1 optical plane. If one extrapolates the relative proportion of Population A/B sources to the whole sample of  $n=1770$  (see the previous section), the radio-loudness probability would be 10% and 2% for Population B and A respectively. A quasar is approximately  $4\times$  more likely to be RL if it shows a Population B optical spectrum. The scarcity of RL quasars in the population A domain is not in dispute. Recent studies (Komossa et al. 2006) searching for RL Narrow-Line Seyfert 1 (NLSy1) sources (extreme population A QSOs with  $\text{FWHM } H\beta \leq 2000 \text{ km s}^{-1}$ ) find that most so-called RL NLSy1 are in fact RI QSOs. A very small number of *bona fide* RL NLSy1 is known at this time (e.g. Zhou & Wang 2002; Zhou et al. 2003, 2006; Komossa et al. 2006).

## 8 DISCUSSION

One of the most fundamental differences among the broad line QSOs involves the existence of RQ and RL populations. Do all sources pass through a RL phase? Do RL quasars represent in some way a physically distinct class? The latter question motivates the high level of interest in the possibility of a RQ/RL dichotomy. We have shown that plots in terms of radio and bolometric luminosity (Figures 6-8) are not the best way to answer it. Samples restricted to high  $L_{\text{bol}}$  sources show hints of a dichotomy, but more complete samples do not. This is due to the numerical imbalance in the two populations. A complete sample of QSOs contains so many RQ sources that the radio brightest of that population will bridge the gap between RQ and RL.

4DE1 provides a better way to address the problem. A way that is independent of the radio and optical luminosity of sources. 4DE1 suggests that the answer to the latter question may be “yes”. If 4DE1 parameters measure fundamental aspects of BLR kinematics and geometry then we have evidence that the RL quasars (mostly Population B) may be significantly different (§ 4) at a fundamental level from the majority of RQ QSOs which occupy the Population A domain. Taken at face value, the 4DE1 optical plane suggests necessary (yet not sufficient) empirical constraints for developing RL activity. It is important to remember that the RQ-RL separation in 4DE1 is not complete. About 60% of RQ QSOs (Population A) show properties almost never seen in RL sources while about 40% of RQ sources are spectroscopically indistinguishable

from RLs (Population B). In this case Population B RQ sources apparently have the necessary BLR properties for radio loudness but not sufficient to be RL.

One possibility is that population B RQ (and especially RI) sources might be the pre- or post-cursors of the RL phase. However, another scenario is that the population B RQ sources occupying the RL domain simply reflect the overlap of two unrelated AGN sequences. The idea of two distinct populations suggests that something else is a necessary ingredient in AGN physics that manifests/triggers radio loudness; it has been suggested the BH spin (e.g. Wilson & Colbert 1995; Moderski et al. 1998; Meier 2001; Volonteri et al. 2007), the host galaxy morphology (e.g. Capetti & Balamverde 2006; Sikora et al. 2007) and/or its link with the nucleus (e.g. Hamilton et al. 2008), the environment (e.g. Kauffmann et al. 2007). Some more clues could come from an analogy with X-ray binaries (e.g. Maccarone et al. 2003; Jester 2005b; Körding et al. 2006a,b). Those studies suggest that RL quasars are in a distinct accretion mode compared to RQ QSOs. Moreover, for a better understanding of radio-loudness one should also consider the ratio of optical:X-ray emission (i.e. disk:corona relative emission)(Körding et al. 2006b). Future studies can certainly explore these valuable arguments incorporating the empirical data presented here.

The overlap of RL and RQ sources in the Population B domain suggests that population A-B distinction may be more physical than RQ-RL comparisons (see also Boroson 2002). The two populations (A and B) are nominally separated at  $\text{FWHM } H\beta=4000 \text{ km s}^{-1}$  and there are many other forms of evidence that support a boundary near this value (Sulentic et al. 2007). We suggested that this might correspond to a critical Eddington ratio ( $\log L/L_{\text{Edd}} \sim 0.15$ ) where the BLR properties change rather suddenly (e.g. Sulentic et al. 2000b; Marziani et al. 2001, 2003b, 2006; Sulentic et al. 2007). In a recent study (Kelly et al. 2008, with reference to Bonning et al. 2007) argue that  $L_{\text{bol}}/L_{\text{Edd}} \approx 0.3$  could indicate some critical change in the accretion disk structure. At this time we can only add that all objects in our sample that have  $L_{\text{bol}}/L_{\text{Edd}}$  larger than this value are exclusively part of the Population A while all others showing  $L_{\text{bol}}/L_{\text{Edd}}$  less than 0.3 are a mixture of Population A and B.

Comparing median  $\text{FWHM } H\beta$  values for FRII and CD RL sources gives 6750 and 4400  $\text{km s}^{-1}$  respectively. This difference is interpreted as a manifestation of source orientation. CDs viewed as near disk face-on (alternatively jet-aligned) sources show  $\text{FWHM}$  measures that are not dominated by Keplerian motions in contrast to FRII quasars. Detection of this FRII-CD difference in median  $\text{FWHM}$  (see also Rokaki et al. 2003; Sulentic et al. 2003; deVries et al. 2006) supports BLR models involving a flattened, disk-like geometry (for a more detailed discussion on BLR structure and dynamics see section 3.1 in Collin et al. 2006). The results on the relative distribution of RQ, as well as FRII and CD RLs, in Figure 4 indicate that face-on RL sources contain a significant extra ( $\sim 2\text{-}3000 \text{ km s}^{-1}$ ) component of line-of sight motion that is not present in face-on RQ AGN. That may or may not be associated with the radio jets.

### 8.1 Radio Intermediates

Armed with evidence that BLR structure in RQ and RL sources may be fundamentally different we return to the sources with  $\log L_{1.4\text{GHz}} \sim 31.0\text{-}31.6 \text{ erg s}^{-1} \text{ Hz}^{-1}$ . They are one, or some combination, of the following: a) radio-weakest RLs, b) radio-strongest RQs or c) a special class (RI) of sources. We disfavor interpre-

tation a) because we find no bona-fide FR II radio morphologies among them. We favor option b) because they show CD emission (like RQs), but cannot be boosted FR IIs. Claims of relativistic jet detection (e.g. Blundell & Beasley 1998) in some of these quasars has led to the suggestion that they might be boosted RQ (option b) sources (e.g. Miller et al. 1993; Falcke et al. 1996a; Wang et al. 2006), which would even more effectively bridge the gap between the majority of RQ sources and the RL quasars. Since the RI show no obvious difference from weaker and unambiguously RQ sources we disfavor option c) and again favor option b).

It has also been proposed that the radio emission in RQs (or alternatively, non-RLs) is mostly related to star formation processes (circumnuclear starbursts, supernovae) (e.g. Sopp & Alexander 1991; Terlevich et al. 1992; Miller et al. 1993; Colina & Perez-Olea 1995). This idea appears to be naturally related to the fact that RQ sources follow the radio-FIR correlation, as mentioned earlier. On the other hand, the discovery of flat radio spectra, elongated radio cores in non-RL quasars and/or high brightness temperatures (e.g. Falcke et al. 1996a; Blundell & Beasley 1998; Wang et al. 2006; Leipski et al. 2006) favors the hypothesis that the mechanism of radio emission in non-RLs is similar to that of RLs. However, the claim of a relativistic jet in “RQ” PG1407+265 (Blundell et al. 2003) involves an unambiguously RL quasar by our definition ( $\log L_{1.4\text{GHz}} = 32.5 \text{ erg s}^{-1} \text{ Hz}^{-1}$ ). Another deep search (Ulvestad et al. 2005) failed to confirm some of the other detections in Blundell & Beasley (1998) indicating that the frequency of occurrence of weak jets in RQ quasars is still uncertain. Some of the claims involve AGN that do not show Type 1 spectra (e.g. Falcke et al. 2000; Nagar et al. 2000, 2001; García-Baretto et al. 2002), which are not considered here.

All RI sources show core (or core-jet) morphology leading us to conclude that their radio emission may be fundamentally different from the classical RL sources (option c?). They could be frustrated jets that face too much resistance from the ambient medium, thus failing to manifest as large scale FR II structures. They cannot be boosted classical RLs unless we have missed a *significant* unboosted FR II population which would presumably lie in the zone of our RI sample. Our comparison of NVSS and FIRST fluxes for the RI sample does not allow us to rule out the existence of hidden FR IIs. A total of  $n=37$  RI were detected in both radio surveys and we find about 18 QSOs with an NVSS flux density excess in the 10-50% range. Some of these involves unrelated point sources within the NVSS beam. A complementary approach is to look for unusual radio structures in the FIRST and NVSS maps.

Table 3 summarizes the properties of quasars showing unusual radio structure. Three of these sources likely involve weak FR II structure while the rest show no hint of it. These three sources are marked with an X in Figure 6. Their location along the trend described by the bona-fide FR IIs increases the likelihood that they may be very weak FR IIs.

Since they are not classical RL sources some of the RI might be pre- and/or post-cursors of the classical RL phenomenon. Support for this interpretation might come from observations showing a flat or curved radio spectra (Falcke et al. 1996a; O’Dea 1998). Sources in this restricted regime merit multifrequency radio measures. The most interesting RI source in this context involves SDSS J232721.97+152437.3 (Table 3) that is indicated with an “X” in Figure 5. It is RI based on an integrated radio luminosity  $\log L_{1.4\text{GHz}} = 31.2 \text{ erg s}^{-1} \text{ Hz}^{-1}$ . The NVSS radio map shows very extended weak lobes and a strong core (NVSS core/lobe  $\sim 3.4$ ). It was not observed by FIRST but it is unlikely that FIRST would have detected the very extended lobes. The low surface brightness

in these lobes may be the signature of a past episode of RL activity with the bright core possibly indicating a renewed phase of radio activity. We may be observing this source between radio outbursts when old decaying lobes can still be detected. A possibly related RL analog involves SDSS J110538.99+020257.4. FIRST detects a strong core elongated  $\sim 45^\circ$  to the direction of very low surface brightness lobes, only one bright enough to be listed in the FIRST source catalog. This is likely another example of a two-phase RL with very old and very young lobe structures. Without doubt a few RI and/or RQ involve weak lobes but there is no evidence for a large population that could boost many CD sources in the range  $\log L_{1.4\text{GHz}} = 31.0\text{--}31.6 \text{ erg s}^{-1} \text{ Hz}^{-1}$ . Or one could extend this range to include all of the so-called RL CDs fainter than  $\log L_{1.4\text{GHz}} \sim 32.5$ . Deeper maps (e.g. PG 1309+355 in Falcke et al. 1996b; Ulvestad et al. 2005) have failed to turn up weak lobe structures.

The RL boundary is also similar to the FRI/FR II break at  $\sim \log L_{1.4\text{GHz}} = 32 \text{ erg s}^{-1} \text{ Hz}^{-1}$  (Owen & Laing 1989). It is important to point out that the FRI/FR II break is not a sharp one and may be a function of optical as well as radio luminosity (Owen & White 1991; Ledlow & Owen 1996). The recent deep radio survey of RQ quasars (Leipski et al. 2006) revealed several RQs with elongated, complex and even double sided structures. One source (out of 14) shows (VLA B-array) structure (PG0026+129) reminiscent of FRI morphology but on a very small ( $\sim 1.5$  kpc) scale and is 1.5 orders of magnitude less radio luminous than the weakest FR II in our RL sample leading us to conclude that this level of activity is unrelated to the classical RL activity. FRI sources are essentially absent from our type 1 QSO sample. We found no FRI structures on FIRST and NVSS maps for any of our RL/RI/RQ sources (Table 3).

## 8.2 Biases?

Is there a chance that we missed some RI, or especially RL QSOs, in Population A? These could expand the RL domain in Figure 4 lessening the strong RQ-RL difference that we found. As pointed out before we should have detected all RI and RL sources in our optically selected SDSS samples. We consider four possible sources of bias in this study.

a) It is known that SDSS is biased against very narrow broad emission line QSOs (often called Narrow Line Seyfert 1’s=NLSy1s) because at least one line with  $\text{FWHM} > 1000 \text{ km s}^{-1}$  is required to be assigned QSO type. We attempted to identify all such extreme NLSy1 sources within our redshift and magnitude limits that are assigned “Galaxy” type by the SDSS spectroscopic pipeline<sup>10</sup>. We found 97 sources with  $\text{psf } g < 17.5$  or  $\text{psf } i < 17.5$  (see Table 2) and only one is clearly RL (SDSS J150324.77+475829.6, but it shows a spectrum with a continuum in high phase and almost missing  $H\beta$ ) and one is RI (SDSS J163323.58+471858.9). One of these sources actually shows the broadest known  $\text{FWHM } H\beta$  ( $\sim 40000 \text{ km s}^{-1}$ , Wang et al. 2005) which exceeded the comprehension of the SDSS broad line identifier. These population A sources clearly show a small probability of radio-loudness. Eventual addition of such NLSy1 sources (our template could not reduce them properly) would increase the RQ-RL domain occupation difference discussed in § 4.

b) SDSS is also apparently biased against steep-spectrum

<sup>10</sup> For such a task we used the SQL (Structured Query Language), instead of a direct selection through the Spectroscopic Query Form of SDSS; in the Appendix we reproduce the “where” clause we formulated.

**Table 5.** Radio Quiet and Intermediate sources in our sample that show peculiar radio morphology.

Name	Comments
SDSS J110717.77+080438.2	galaxy nearby; core-jet morphology
SDSS J114047.9+462204.8	misaligned nearby radio structure with no SDSS-detected counterpart
SDSS J120014.08-004638.7	possible core+lobes structure
SDSS J171322.58+325627.9	possible lobes
SDSS J230443.47-084108.6	RQ with elongation
	on either side of the radio core
SDSS J232721.96+152437.3	not in FIRST catalog;
	NVSS shows extended weak lobes

lobe-dominated quasars (Richards et al. 2002). There is no reason to assume that any missed FRII would preferentially populate region A in 4DE1. We tried to avoid missing RL sources with largely separated radio lobes and no radio detected core between them by carefully examining FIRST and NVSS radio maps. We consider that our approach is very effective in turning up all FRIIs without a detected radio-core at/near the position of quasar.

c) We must also consider that SDSS does not include sources brighter than  $i \sim 15.0$ . This is a technical limitation imposed to avoid contamination of adjacent fibers by very bright sources. How would the omission of these bright (mostly low luminosity Seyferts) AGN affect our conclusions? The latest incarnation of the 4DE1 spectroscopic Atlas (Marziani et al. 2003a) includes 215 objects of which 61 are brighter than  $V=15.0$  (4 RL) and 21 are brighter than  $V=14.0$  (3 RL). 56/61 objects show  $z < 0.1$  (41/61 with  $z < 0.05$ ). Most of these objects (53) show bolometric luminosity  $\log L_{bol} > 44.0 \text{ erg s}^{-1}$ , which according to Figure 6 are bright enough to be RL. The RL percentage ( $\sim 7\%$ ) suggests that SDSS exclusion of such bright AGN will not affect our conclusions.

d) As mentioned earlier we have a total sample size of  $n=1770$  QSOs brighter than  $\text{psf } g=17.5$  or  $\text{psf } i=17.5$ . We have almost complete spectroscopic coverage for all RL and RI sources in this range meaning that we extracted reliable 4DE1 parameters for use in Figures 4 and 5. Similar parameters were extracted for  $n=333$   $\text{psf } g$  selected RQ quasars. Would inclusion of fainter  $\text{psf } g$  selected and the many  $\text{psf } i$  selected RQ sources change our 4DE1 definition/domain of RQ? We think the answer is clearly “no” for several reasons: 1) a random sample of 333 RQ is sufficient to define the general properties of the RQ parent population, 2) the RQ domain defined with the SDSS sample is very similar to that defined from our Atlas sample (Marziani et al. 2003a; Sulentic et al. 2007) that shows only partial overlap with SDSS, 3) recent VLT spectroscopy of the  $H\beta$  region in high  $z$  sources (Sulentic et al. 2004, 2006; Marziani et al. 2008) again show the same trends as for the low redshift samples. The  $\text{psf } i$  selected quasars (fainter than  $\text{psf } g=17.5$ ) show too low S/N to allow accurate 4DE1 measures to be extracted. They are in addition strongly host galaxy contaminated as a class. Random examination of these noisy spectra give no evidence that they would change the general RQ properties derived from the brighter sources.

### 8.3 Black Hole Mass and Radio Loudness

The results of Figure 4 indicate that the vast majority of RL sources show  $\text{FWHM } H\beta > 4000 \text{ km s}^{-1}$ , with the median  $\text{FWHM } H\beta$  of the FRII population (viewed as inclined RL sources) near  $6750 \text{ km s}^{-1}$ . Using  $\text{FWHM } H\beta$  and  $L_{5100\text{\AA}}$  measures to estimate black

hole masses and  $L_{bol}/L_{Edd}$  values implies that  $M_{BH} > 1 \times 10^8 M_{\odot}$  for RL sources, with a strong concentration between  $3 \times 10^8$  and  $3 \times 10^9 M_{\odot}$  (Marziani et al. 2003b; Sulentic et al. 2006). Eddington ratios for RL sources are restricted to  $L_{bol}/L_{Edd} < 0.15-0.30$  (see previous discussion). The RQ majority show generally smaller values of  $M_{BH}$  and larger values of  $L_{bol}/L_{Edd}$  (e.g. Boroson 2002; Marziani et al. 2003b; Dunlop et al. 2003; McLure & Jarvis 2004; Metcalf & Magliocchetti 2006). However, some studies (e.g. K rding et al. 2006b) suggest that radio-loudness is not directly related to a single variable like  $M_{BH}$  or accretion rate.

RL/RQ comparisons using spectral properties are sensitive to the relative contributions of Population A/B RQ sources in the sample under study. RQ Population B sources will show masses and Eddington ratios similar to RL sources while the majority of RQ sources (Population A) will not. The numbers quoted here come from analysis of our Atlas sample (Marziani et al. 2003a; Sulentic et al. 2006). Preliminary analysis of the SDSS sample (e.g. Figure 4) indicate that the conclusions will be very similar to those summarized here (see also Laor 2003 for some relevant comments).

A full discussion and comparison with other studies will be given in a later paper (Zamfir et al. 2008). We emphasize the importance of using adequate S/N spectra and proper identification/subtraction of narrow  $H\beta$  for estimating black hole masses and Eddington ratios in AGN.

## 9 CONCLUSIONS

Three criteria have been used to isolate RL quasar samples from the RQ majority: 1) radio/optical flux density ratios (e.g.  $R_K$  as defined in § 1), 2) radio luminosity and 3) radio morphology. The first criterion is the least precise and was not used in this study. We used a combination of criteria 2 and 3 which involved determining the cutoff from the radio luminosities of the weakest FRII sources using one of the most complete RL samples ever compiled. The cutoff value  $\log L_{1.4\text{GHz}} = 31.6 \text{ ergs s}^{-1} \text{ Hz}^{-1}$  agrees closely with the value derived in an earlier attempt using a more heterogeneous sample. We think this value is therefore a robust boundary for the classical RL phenomenon. We find many CD RL sources that are RL by this definition but are on the low luminosity side of most FRII sources. These RL CD sources cannot be FRII sources viewed jet-on and are either boosted RQ quasars or precursors of the RL phenomenon.

We find that RQ-RL comparisons involving radio and bolometric luminosity (diagrams) yield ambiguous results about the reality of a RQ-RL dichotomy. A gap or dichotomy between the two populations is filled by the radio bright end of the RQ source distri-

bution and possible radio pre- and/or post-cursors in the zone of RI (and RL) sources. The optical diagnostic plane of 4DE1 provides much less ambiguous evidence that RL show significant structural and kinematic differences from the majority of RQ sources which is consistent with a real dichotomy. 4DE1 also shows that RI and RQ sources are spectroscopically indistinguishable. Our Type 1 QSO sample shows no evidence for an FRI population within the radio resolution constraints of NVSS/FIRST.

## ACKNOWLEDGMENTS

S. Zamfir acknowledges support from the Graduate Council Research/Creative Activity Fellowship offered by the Graduate School of the University of Alabama for the 2007/2008 academic year. S. Zamfir and J. W. Sulentic kindly acknowledge the hospitality of Asiago Observatory (Italy) in the summer of 2006, when this project was outlined. The authors thank the reviewer, Dr. Sebastian Jester, for numerous comments and suggestions, which certainly improved the quality of the paper.

Funding for the SDSS and SDSS-II has been provided by the Alfred P. Sloan Foundation, the Participating Institutions, the National Science Foundation, the U.S. Department of Energy, the National Aeronautics and Space Administration, the Japanese Monbukagakusho, the Max Planck Society, and the Higher Education Funding Council for England. The SDSS Web Site is <http://www.sdss.org/>. The SDSS is managed by the Astrophysical Research Consortium for the Participating Institutions. The Participating Institutions are the American Museum of Natural History, Astrophysical Institute Potsdam, University of Basel, University of Cambridge, Case Western Reserve University, University of Chicago, Drexel University, Fermilab, the Institute for Advanced Study, the Japan Participation Group, Johns Hopkins University, the Joint Institute for Nuclear Astrophysics, the Kavli Institute for Particle Astrophysics and Cosmology, the Korean Scientist Group, the Chinese Academy of Sciences (LAMOST), Los Alamos National Laboratory, the Max-Planck-Institute for Astronomy (MPIA), the Max-Planck-Institute for Astrophysics (MPA), New Mexico State University, Ohio State University, University of Pittsburgh, University of Portsmouth, Princeton University, the United States Naval Observatory, and the University of Washington.

This research has made use of the NASA/IPAC Extragalactic Database (NED) which is operated by the Jet Propulsion Laboratory, California Institute of Technology, under contract with the National Aeronautics and Space Administration.

## REFERENCES

- Adelman-McCarthy, J.K. et al. 2007, *ApJS*, 172, 634  
 Barthel, P. D. 1989, *ApJ*, 336, 606  
 Becker, R. H., White, R. L., Helfand, D. J. 1995, *ApJ*, 450, 559  
 Blundell, K. M. & Beasley, A. J. 1998, *MNRAS*, 299, 165  
 Blundell, K. M. & Rawlings, S. 2001, *ApJ*, 562, L5  
 Blundell, K. M., Beasley, A. J., Bicknell, G. V. 2003, *ApJ*, 591, L103  
 Bonning, E. W., Cheng, L., Shields, G. A., Salviander, S., Gebhardt, K. 2007, *ApJ*, 659, 211  
 Boroson, T. A. & Green, R. F. 1992, *ApJS*, 80, 109  
 Boroson, T. A. 2002, *ApJ*, 565, 78  
 Boyle, B. J., Shanks, T., Croom, S. M., Smith, R. J., Miller, L., Loaring, N., Heymans, C. 2000, *MNRAS*, 317, 1014  
 Brotherton, M. S., Tran, H. D., Becker, R. H., Gregg, M. D., Laurent-Muehleisen, S. A., White, R. L. 2001, *ApJ*, 546, 775  
 Bruzual, G. & Charlot, S. 2003, *MNRAS*, 344, 100  
 Capetti, A. & Balmaverde, B. 2006, *A&A*, 453, 27  
 Cirasuolo, M., Magliocchetti, M., Celotti, A., Danese, L. 2003a, *MNRAS*, 341, 993  
 Cirasuolo, M., Celotti, A., Magliocchetti, M., Danese, L. 2003b, *MNRAS*, 346, 447  
 Colina, L. & Perez-Olea, D. E. 1995, *MNRAS*, 277, 845  
 Collin, S., Kawaguchi, T., Peterson, B. M., Vestergaard, M. 2006, *A&A*, 456, 75  
 Condon, J. J. 1992, *ARA&A*, 30, 576  
 Condon, J. J., Cotton, W. D., Greisen, E. W., Yin, Q. F., Perley, R. A., Taylor, G., Broderick, J. J. 1998, *AJ*, 115, 1693  
 Croom, S. M., Smith, R. J., Boyle, B. J., Shanks, T., Miller, L., Outram, P. J., Loaring, N. S. 2004, *MNRAS*, 349, 1397  
 de Vries, W. H., Becker, R. H., White, R. L. 2006, *AJ*, 131, 666  
 Dunlop, J. S., McLure, R. J., Kukula, M. J., Baum, S. A., O'Dea, C. P., Hughes, D. H. 2003, *MNRAS*, 340, 1095  
 Falcke, H., Sherwood, W., Patnaik, A.R. 1996a, *ApJ*, 471, 106  
 Falcke, H., Sherwood, W., Patnaik, A.R. 1996b, *ApJ*, 473, L13  
 Falcke, H., Nagar, N. M., Wilson, A. S., Ulvestad, J. S. 2000, *ApJ*, 542, 197  
 Fanaroff, B. L. & Riley, J. M. 1974, *MNRAS*, 167, 31  
 Fasano, G. & Franceschini, A. 1987, *MNRAS*, 225, 155  
 García-Barreto, J. A., Franco, J., Rudnick, L. 2002, *AJ*, 123, 1913  
 Gopal-Krishna & Wiita, P. J. 2000, *A&A*, 363, 507  
 Goldschmidt, P., Kukula, M. J., Miller, L., Dunlop, J. S. 1999, *ApJ*, 511, 612  
 Green, R. F., Schmidt, M., Liebert, J. 1986, *ApJS*, 61, 305  
 Haas, M., Klaas, U., Müller, S. A. H., Bertoldi, F., Camenzind, M., Chini, R., Krause, O., Lemke, D., Meisenheimer, K., Richards, P. J., Wilkes, B. J. 2003, *A&A*, 402, 87  
 Hamilton, T. S., Casertano, S., Turnshek, D. A. - 2008, *arXiv:0802.1786*  
 Heywood, I., Blundell, K. M., Rawlings, S. 2007, *MNRAS*, 381, 1093  
 Hooper, E. J., Impey, C. D., Foltz, C. B., Hewett, P. C. 1995, *ApJ*, 445, 62  
 Ho, L. C. & Peng, C. Y. 2001, *ApJ*, 555, 650  
 Hogg, D. W. - 1999, *astro-ph/9905116*  
 Hopkins, P. F., Richards, G. T., Hernquist, L. 2007, *ApJ*, 654, 731  
 Ivezić et al. 2002, *AJ*, 124, 2364  
 Jackson, C. A. & Wall, J. V. 1999, *MNRAS*, 304, 160  
 Jester et al. 2005a, *AJ*, 130, 873  
 Jester, S. 2005b, *ApJ*, 625, 667  
 Jiang, L., Fan, X., Ivezić, Ž., Richards, G. T., Schneider, D. P., Strauss, M. A., Kelly, B. C. 2007, *ApJ*, 656, 680  
 Kauffmann, G., Heckman, T. M., Best, P. N. - 2007, *arXiv:0709.2911*  
 Kellermann, K. I., Sramek, R., Schmidt, M., Shaffer, D. B., Green, R. 1989, *AJ*, 98, 1195  
 Kellermann, K. I., Sramek, R. A., Schmidt, M., Green, R. F., Shaffer, D. B. 1994, *AJ*, 108, 1163  
 Kelly, B. C., Bechtold, J., Trump, J. R., Vestergaard, M. - 2008, *arXiv:0801.2383*  
 Komossa, S., Voges, W., Xu, D., Mathur, S., Adorf, H.-M., Lemson, G., Duschl, W. J., Grupe, D. 2006 *AJ*, 132, 531  
 Körding, E. G., Fender, R. P., Migliari, S. 2006a, *MNRAS*, 369, 1451



- Körding, E. G., Jester, S., Fender, R. 2006b, MNRAS, 372, 1366
- Körding, E. G., Jester, S., Fender, R. 2008, MNRAS, 383, 277
- Kukula, M. J., Dunlop, J. S., Hughes, D. H., Rawlings, S. 1998, MNRAS, 297, 366
- Lacy, M., Laurent-Muehleisen, S. A., Ridgway, S. E., Becker, R. H., White, R. L. 2001, ApJ, 551, L17
- Labita, M., Treves, A., Falomo, R. 2007 - arXiv:0710.5035
- Laor, A. 2003 - astro-ph/0312417
- Ledlow, M. J. & Owen, F. N. 1996, AJ, 112, 9
- Leipski, C., Falcke, H., Bennert, N., Hüttemeister, S. 2006, A&A, 455, 161
- Lipari, S., Terlevich, R., Macchetto, F. 1993, ApJ, 406, 451
- Liu, Y., Jiang, D. R., Gu, M. F. 2006, ApJ, 637, 669
- Liu, Y. & Zhang, S. N. 2007, ApJ, 667, 724
- Lu, Y., Wang, T., Zhou, H., Wu, J. 2007, AJ, 133, 1615
- Maccarone, T. J., Gallo, E., Fender, R. 2003, MNRAS, 345, L19
- Marziani, P., Sulentic, J. W., Zwitter, T., Dultzin-Hacyan, D., Calvani, M. 2001, ApJ, 558, 553
- Marziani, P., Sulentic, J. W., Zamanov, R., Calvani, M., Dultzin-Hacyan, D., Bachev, R., Zwitter, T. 2003a, ApJS, 145, 199
- Marziani, P., Zamanov, R. K., Sulentic, J. W., Calvani, M. 2003b, MNRAS, 345, 1133
- Marziani, P., Dultzin-Hacyan, D., Sulentic, J. W. - New Developments in Black Hole Research, edited by Paul V. Kreidler, 2006 - astro-ph/0606678
- Marziani, P. et al. 2008 - in preparation
- McLure, R. J., Kukula, M. J., Dunlop, J. S., Baum, S. A., O'Dea, C. P., Hughes, D. H. 1999, MNRAS, 308, 377
- McLure, R. J. & Jarvis, M. J. 2004, MNRAS, 353, L45
- Meier, D. L. 2001, ApJ, 548, L9
- Metcalfe, R. B. & Magliocchetti, M. 2006, MNRAS, 365, 101
- Miller, L., Peacock, J. A., Mead, A. R. G. 1990, MNRAS, 244, 207
- Miller, P., Rawlings, S., Saunders, R. 1993, MNRAS, 263, 425
- Moderski, R., Sikora, M., Lasota, J.-P. 1998, MNRAS, 301, 142
- Nagar, N. M., Falcke, H., Wilson, A. S., Ho, L. C. 2000, ApJ, 542, 186
- Nagar, N. M., Wilson, A. S., Falcke, H. 2001, ApJ, 559, L87
- O'Dea, C. P. 1998, PASP, 110, 493
- Orr, M. J. L. & Browne, I. W. A. 1982, MNRAS, 200, 1067
- Owen, F. N. & Laing, R. A. 1989, MNRAS, 238, 357
- Owen, F. N. & White, R. A. 1991, MNRAS, 249, 164
- Padovani, P. 1993, MNRAS, 263, 461
- Peacock, J. A. 1983, MNRAS, 202, 615
- Peacock, J. A., Miller, L., Longair, M. S. 1986, MNRAS, 218, 265
- Rawlings, S. & Saunders, R. 1991, Nature, 349, 138
- Richards, G. T. et al. 2002, AJ, 123, 2945
- Richards, G. T. et al. 2003, AJ, 126, 1131
- Richards, G. T. et al. 2005, MNRAS, 360, 839
- Richards, G. T. et al. 2006, AJ, 131, 2766
- Rokaki, E., Lawrence, A., Economou, F., Mastichiadis, A. 2003, MNRAS, 340, 1298
- Scheuer, P. A. G. 1987 in Proceedings of the Workshop, Pasadena, CA, Oct. 28-30, 1986 (A88-39751 16-90). Cambridge and New York, Cambridge University Press, p. 104-113, Zensus, J. A., Pearson, T. J. eds.
- Schmidt, M. & Green, R. F. 1983, ApJ, 269, 352
- Schneider et al. 2007, AJ, 134, 102
- Serjeant, S., Rawlings, S., Lacy, M., Maddox, S. J., Baker, J. C., Clements, D. 1998, MNRAS, 194, 494
- Sikora, M., Stawarz, Ł., Lasota, J.-P. 2007, ApJ, 658, 815
- Sopp, H. M. & Alexander, P. 1991, MNRAS, 251, 14
- Stocke, J. T., Morris, S. L., Weymann, R. J., Foltz, C. B. 1992, ApJ, 396, 487
- Sulentic, J. W., Zwitter, T., Marziani, P., Dultzin-Hacyan, D. 2000a, ApJ, 536, L5
- Sulentic, J. W., Marziani, P., Dultzin-Hacyan, D. 2000b, ARA&A, 38, 521
- Sulentic, J. W., Zamfir, S., Marziani, P., Bachev, R., Calvani, M., Dultzin-Hacyan, D. 2003, ApJ, 597, L17
- Sulentic, J. W., Stirpe, G. M., Marziani, P., Zamanov, R., Calvani, M., Braito, V. 2004, A&A, 423, 121
- Sulentic, J. W., Repetto, P., Stirpe, G. M., Marziani, P., Dultzin-Hacyan, D., Calvani, M. 2006, A&A, 456, 929
- Sulentic, J. W., Bachev, R., Marziani, P., Alenka Negrete, C., Dultzin, D. 2007, ApJ, 666, 757
- Taylor, G. L., Dunlop, J. S., Hughes, D. H., Robson, E. I. 1996, MNRAS, 283, 930
- Terlevich, R., Tenorio-Tagle, G., Franco, J., Melnick, J. 1992, MNRAS, 255, 713
- Terashima, Y. & Wilson, A. S. 2003, ApJ, 583, 145
- Ulvstad, J. S., Antonucci, R. R. J., Barvainis, R. 2005, ApJ, 621, 123
- Urry, C. M. & Padovani, P. 1995, PASP, 107, 803
- Vanden Berk, D. E. et al. 2005, AJ, 129, 2047
- Vanden Berk, D. E. et al. 2006, AJ, 131, 84
- Véron-Cetty, M.-P., Joly, M., Véron, P., Boroson, T., Lipari, S., Ogle, P. 2006, A&A, 451, 851
- Visnovsky, K. L., Impey, C. D., Foltz, C. B., Hewett, P. C., Weymann, R. J., Morris, S. L. 1992, ApJ, 391, 560
- Volonteri, M., Sikora, M., Lasota, J.-P. 2007, ApJ, 667, 704
- Wadadekar, Y. & Kembhavi, A. 1999, AJ, 118, 1435
- Wang, T.-G., Dong, X.-B., Zhang, X.-G., Zhou, H.-Y., Wang, J.-X., Lu, Y.-J. 2005, ApJ, 625, L35
- Wang, T.-G., Zhou, H.-Y., Wang, J.-X., Lu, Y.-J., Lu, Y. 2006, ApJ, 645, 856
- White, R. L. et al. 2000, ApJS, 126, 133
- White, R. L., Helfand, D. J., Becker, R. H., Glikman, E., deVries, W. 2007, ApJ, 654, 99
- Willott, C. J., Rawlings, S., Blundell, K. M., Lacy, M. 1998, MNRAS, 300, 625
- Willott, C. J., Rawlings, S., Blundell, K. M., Lacy, M., Eales, S. A. 2001, MNRAS, 322, 536
- Wilson, A. S. & Colbert, E. J. M. 1995, ApJ, 438, 62
- Xu, C., Livio, M., Baum, S. 1999, AJ, 118, 1169
- Yun, M. S., Reddy, N. A., Condon, J. J. 2001, ApJ, 554, 803
- Zamfir, S. et al. 2008 - in preparation
- Zhou, H.-Y. & Wang, T.-G. 2002, ChJAA, 2, 501
- Zhou, H.-Y., Wang, T.-G., Dong, X.-B., Zhou, Y.-Y., Li, C. 2003, ApJ, 584, 147
- Zhou, H., Wang, T., Yuan, W., Lu, H., Dong, X., Wang, J., Lu, Y. 2006, ApJS, 166, 128

#### APPENDIX A: AN SQL SEARCH FOR QSO WITH FWHM $H\beta < 1000 \text{ km s}^{-1}$ IN DR5

We reproduce here the “where” clause we formulate to isolate objects labeled “Galaxy” by the spectroscopic algorithm of SDSS (DR5); their spectra show  $H\beta$  emission line narrower than  $1000 \text{ km s}^{-1}$  in the sources rest frame. The  $\sigma$  interval required in the query would translate into an *observed* FWHM  $H\beta$  range  $\sim 300\text{--}1700 \text{ km s}^{-1}$ . This takes into account the  $(1+z)$  scaling of line width from

source's frame to the observed frame, e.g. a rest frame FWHM  $H\beta$  =  $1000 \text{ km s}^{-1}$  would be observed from  $z=0.7$  as  $1700 \text{ km s}^{-1}$ .

```
SELECT ... FROM SpecPhoto as S,
        SpecLine as L
WHERE
    S.SpecObjID = L.SpecObjID and
    L.LineId = 4863 and
    S.z <= 0.7 and
    L.ew > 0 and
    L.sigma <= 11.7 and
    L.sigma >= 2.1 and
    S.psfMag_g <= 17.5
```

The spectra selected this way have been visually examined and we kept only the bona-fide Type 1 QSO for our statistical estimates, as explained in the text. We selected “Galaxy” spectra based on psf  $i$  magnitude cut replacing the last line in the “where” clause above with:

```
S.psfMag_i <= 17.5
```